Mixed carbonate-siliciclastic contourite drift deposits associated with the entrance of an Atlantic-Mediterranean corridor (late Miocene, southwest Spain)

J. Reolid *, J. Aguirre, J.N. Pérez-Asensio, Á. Puga-Bernabéu, J.C. Braga, J.M. Martín

Departamento de Estratigrafía y Paleontología, Universidad de Granada, Avenida de la Fuente Nueva SN, 18071 Granada, Spain

ARTICLE INFO

ABSTRACT

Carbonate contourite drifts are poorly documented in the onshore record because of the difficulty of implementing diagnostic criteria for their recognition. Accordingly, little is known about the relative position of carbonate drifts with respect to ancient carbonate platforms, seaways and shallow passages within the context of palaeoceanography. This study presents a fossil example of mixed carbonate-siliciclastic drift cropping out in a quarry in Osuna (Sevilla province, southern Spain) at the northern end of the Guadalhorce Corridor, a Miocene strait connecting the Mediterranean Sea and the Atlantic Ocean in the Betic Cordillera. Based on the facies and sedimentary structures, the studied succession is divided into three units: 1) the lower unit, Unit 1, is a 33-m thick succession of large carbonate bodies with mega cross-stratification pointing to the southeast and secondarily to the northwest interpreted as a contourite drift; 2) the intermediate Unit 2 is a 0.5–2-m thick terrigenous conglomerate body eroding the top of Unit 1; and 3) the uppermost Unit 3 consists of a 6-m thick siliciclastic-dominated succession with herringbone cross-stratification and a dominant direction of the structures to the northwest interpreted as tidal deposits. The large-scale sediment bodies with mega cross-beds, the presence of reactivation surfaces with grain-size changes, and the unidirectionality of the structures were diagnostic for the recognition of Unit 1 as drift deposits. The dominant sedimentary structures pointing to the southeast in the drift were generated by Atlantic inflow into the Mediterranean. This challenges the classical "siphon" model for the Atlantic-Mediterranean water-mass circulation pattern for this age. The conglomerates of Unit 2 evidence regional uplift of the southern margin of the Guadalquivir Basin that promoted a change in the depositional mode from a bottom-current dominated (Unit 1) to a tide-dominated environment (Unit 3) after the closure of the Guadalhorce Corridor in the Messinian.

1. Introduction

The action of ocean bottom currents induces selective deposition, as well as sediment winnowing and redistribution. Extensive sediment drifts may form in areas affected by the persistent action of bottom currents. The external morphology and internal architecture of these deposits have been widely studied leading to a synoptic classification based predominantly on siliciclastic drifts (Hernández-Molina et al., 2008; Rebesco et al., 2014; Shanmugam, 2017). Siliciclastic drifts have been reported to record palaeoclimatic and palaeoceanographic conditions at a higher resolution than pelagic background sedimentation (Rebesco, 2005; Rebesco et al., 2014; Shanmugam, 2017; Stow and Smillie, 2020).

In most cases, the identification of a sedimentary succession as a sediment drift relies on the interpretation of reflection seismic data sets where the large-scale geometry is imaged (Anselmetti et al., 2000; Ercilla et al., 2002; Bergman, 2004; Hernandez-Molina et al., 2006; Hernández-Molina et al., 2011, 2013, 2014; Betzler et al., 2014; Chabaud et al., 2016; Lüdmann et al., 2016; Eberli and Betzler, 2019; Paulat et al., 2019). In some cases, the seismic information can be implemented with sediment information from cores and well-logs (Hernández-Molina et al., 2013, 2014; Betzler et al., 2016, 2018; Lüdmann et al., 2018; Eberli and Betzler, 2019; Reolid et al., 2019; de Castro et al., 2021). However, very few studies deal with the problem of recognizing contourite drifts in outcrops, where the characteristic seismic-scale drift geometries are not identifiable (Stow et al., 1998, 2002; Capella et al., 2018; Eberli and Betzler, 2019; Reolid and Betzler, 2019; Reolid et al., 2021; Hüneke et al., 2020; de Weger et al., 2021). Contourite drift outcrops are, in fact, only scarcely recognised. This generally resulted in the lack of distinct diagnostic drift features and the underrepresentation of contourite drifts in outcrops (Huneke and Stow, 2008; Rebesco et al., 2014; Shanmugam, 2017; Hüneke et al., 2020).

* Corresponding author.
E-mail address: jreolid@ugr.es (J. Reolid).

The main diagnostic criterion for the identification of contourite drift sediments in outcrops is the occurrence of bigradational sequences (Gonthier et al., 1984; Stow and Faugères, 2008). However, this feature is not observable in muddy or sandy contourites where the homogeneity of the sediment does not allow identifying changes in grain size (Shanmugam, 2017; Stow and Smillie, 2020). A high degree of bioturbation is also characteristic of contourite drift deposits, and contributes to the homogenization of the sediment (Wetzel et al., 2008; Rodríguez-Tovar and Hernández-Molina, 2018; Reolid and Betzler, 2019; Reolid et al., 2021; Bialik et al., 2022). In fossil examples cropping out onshore, carbonate drifts show traction sedimentary structures from lenticular and flaser bedding to mega cross-bedding, which are considered indicative of deposition under the action of bottom currents (Stow et al., 1998, 2002; Shanmugam, 2000; Martín-Chivelet et al., 2008; Hüneke et al., 2020; Reolid et al., 2021). However, further examples are still needed to have a good understanding of onshore drift deposits from different settings.

Fossil carbonate drifts are restricted to three main settings: 1) at the flanks of carbonate banks as periplatform drifts (Mullins and Neumann, 1979; Mullins et al., 1980; Betzler et al., 2014; Chabaud et al., 2016); 2) in seaways separating carbonate banks as detached drifts (Anselmetti et al., 2000; Bergman, 2004; Lüdmann et al., 2016; Paulat et al., 2019); and 3) at the down-current end of shallow passages dissecting carbonate banks as delta drifts (Lüdmann et al., 2018; Eberli et al., 2019; Reolid et al., 2019). However, little is known about the relative position of outcropping fossil drifts with respect to ancient carbonate platforms, seaways and shallow passages (Eberli and Betzler, 2019). The aim of this study is to present for the first time an onshore example of a mixed carbonate-siliciclastic drift located at the entrance of a Miocene Betic strait connecting the Atlantic Ocean and the Mediterranean Sea and to reconstruct the palaeoceanographic conditions that led to its formation.

The nearly complete separation of the Mediterranean from the Atlantic Ocean during the late Miocene (Martín et al., 2001, 2009, 2010; Betzler et al., 2006; Flecker et al., 2015; Tulbure et al., 2017; Capella et al., 2018; Ng et al., 2021) had a global impact on the thermohaline ocean circulation and, consequently, on the climate and organic matter fluxes (Pérez-Asensio et al., 2012, 2013, 2014; Jiménez-Moreno et al., 2013). In the Betic Cordillera, several straits connected the Mediterranean and the Atlantic throughout the Guadalquivir Basin (Martín et al., 2001, 2009, 2014; Betzler et al., 2006; Puga-Bernabéu et al., 2022). The sedimentary infilling of these marine seaways is characterised by coarse-grained deposits displaying gigantic cross-stratifications (decametres to hectometres in length), generated by the intensification of currents in narrow straits. The study area is located at the northern end of one of these straits at the southern margin of the Guadalquivir Basin, in the central Betic Cordillera.

The results of this research will contribute to expand and improve the existing outcrop criteria for the recognition of contourite drift deposits. The sedimentological and palaeontological information shed light on the bottom current regime and circulation patterns of the ancient water masses in the Atlantic/Mediterranean straits during the Messinian, a period of major palaeocenographic changes in the western Mediterranean leading up to the Messinian Salinity Crisis.

2. Location and geological setting

The study area is located at the southern margin of the Guadalquivir Basin, the foreland basin of the Betic Cordillera (Fig. 1; Braga et al., 2002; García-Castellanos et al., 2002, Larrasoaña Gorosquieta et al., 2019). The Guadalquivir Basin, with a WSW-ENE elongated triangular outline, formed by flexural subsidence related to the stacking of thrust units of the Betic Cordillera caused by the north to northwest convergence of African and Eurasian plates (Martín et al., 2009, 2014; Larrasoaña Gorosquieta et al., 2019). The Neogene sedimentary infilling of the basin was mostly the result of the southeasternwards advancement of shallow- and deep-water deposits along the axis of the basin (González-Delgado et al., 2004; Martínez del Olmo and Martín, 2016;

Reolid et al., 2016a; Martínez del Olmo, 2019). In addition, the stacking of sediments in the Betic front produced instabilities and collapse of large amounts of reworked materials, mostly from the Triassic, that were redeposited in the basin (Martínez del Olmo and Martín, 2016; Martínez del Olmo, 2019). These olistostromic deposits, the Guadalquivir Olistostromic Unit (GOU), crop out extensively at the southern margin of the basin and extend up to its axis below the surface (Divar and Cruz-Sanjulián, 1986). Osuna is a village located at the northern limit of the outcropping GOU, which there consists of Middle Miocene whitish-grey diatomitic marls, regionally known as "moronitas" or "albarizas" (Cruz-Sanjulián, 1975; Divar and Cruz-Sanjulián, 1986).

The abandoned Osuna Quarry is approximately 30 km to the northwest of the northernmost outcrop of the Guadalhorce Corridor (Figs. 1, 2A), and the section is coeval with the deposits filling this gateway. The Guadalhorce Corridor was the last active Atlantic-Mediterranean Betic connection (Martín et al., 2001, 2014). It was a northwest to southeast trending narrow and shallow strait with an estimated maximum width of 5 km and a maximum water depth of about 120 m, developed in a tectonic linear depression produced by northwest to southeast faults (López-Garrido and Sanz de Galdeano, 1999; Martín et al., 2001). All the large-scale sedimentary structures within the Guadalhorce Corridor, including tabular and trough cross-bedding of up to 30 m in set thickness, are indicative of unidirectional traction currents flowing towards the Atlantic with a northwest direction (Martín et al., 2001). The closure of the Guadalhorce Corridor took place in the Messinian (Martín et al., 2001; Pérez-Asensio et al., 2012).

The studied Upper Miocene deposits of the Osuna Quarry mostly consist of mixed siliciclastics and bioclastic carbonates containing abundant nodular and branching bryozoans and small benthic foraminifer remains, with smaller amounts of echinoid, calcareous red algal, and bivalve fragments (Verdenius, 1970). Rhodoliths are also locally present. Two thin silt beds, 10–15-cm thick, intercalate with the carbonates (Fig. 2B). These carbonates constitute the Cantera Member of Verdenius (1970), who emphasised that the absence of planktonic foraminifera prevented dating the Osuna carbonates. He tentatively correlated the Osuna carbonates with the carbonates extensively cropping out in Carmona (Guadaira Formation) 55 km west of Osuna. The carbonates at Carmona have been dated as Messinian (Berggren and Haq, 1976; Aguirre et al., 2015).

2.1. Oceanography and palaeoceanography of the Atlantic-Mediterranean connection

At present, the Mediterranean Sea connects with the Atlantic Ocean through the Strait of Gibraltar, where the water mass exchange is characterised by an anti-estuarine circulation pattern (Wüst, 1961). This means that lower salinity waters from the North Atlantic (the Atlantic Inflow Water; AIW) flow superficially eastwards into the Mediterranean, while dense, saline intermediate and deep Mediterranean waters (the so-called Mediterranean Outflow Water; MOW) flow westward through the straits. The present-day interface between both water masses in the Strait of Gibraltar is located between 180- and 200-m water depth (Soto-Navarro et al., 2010). However, once the inflow crosses the strait the interface between the two water masses rapidly reaches depths between 200 and 300 m (Millot, 2014). The westward currents associated with the MOW originate a large contourite drift system in the Gulf of Cadiz, which is >160 km long at water depths below 600 m (Hernandez-Molina et al., 2006; Hernández-Molina et al., 2011, 2013, 2014). However, there are also contourite drifts developed in the Mediterranean part of the Gibraltar Strait related to the inflow of surface water as is the case of the Ceuta Drift (Ercilla et al., 2002). This Quaternary drift has a minimum water depth of 200 m, which is consistent with the maximum depth of the AIW once it exits the Strait of Gibraltar (Soto-Navarro et al., 2010; Millot, 2014).

During the Miocene, however, the circulation of the two water masses, the MOW and the AIW, was not concentrated through the Strait of Gibraltar but distributed in complex system of corridors in the southern part of
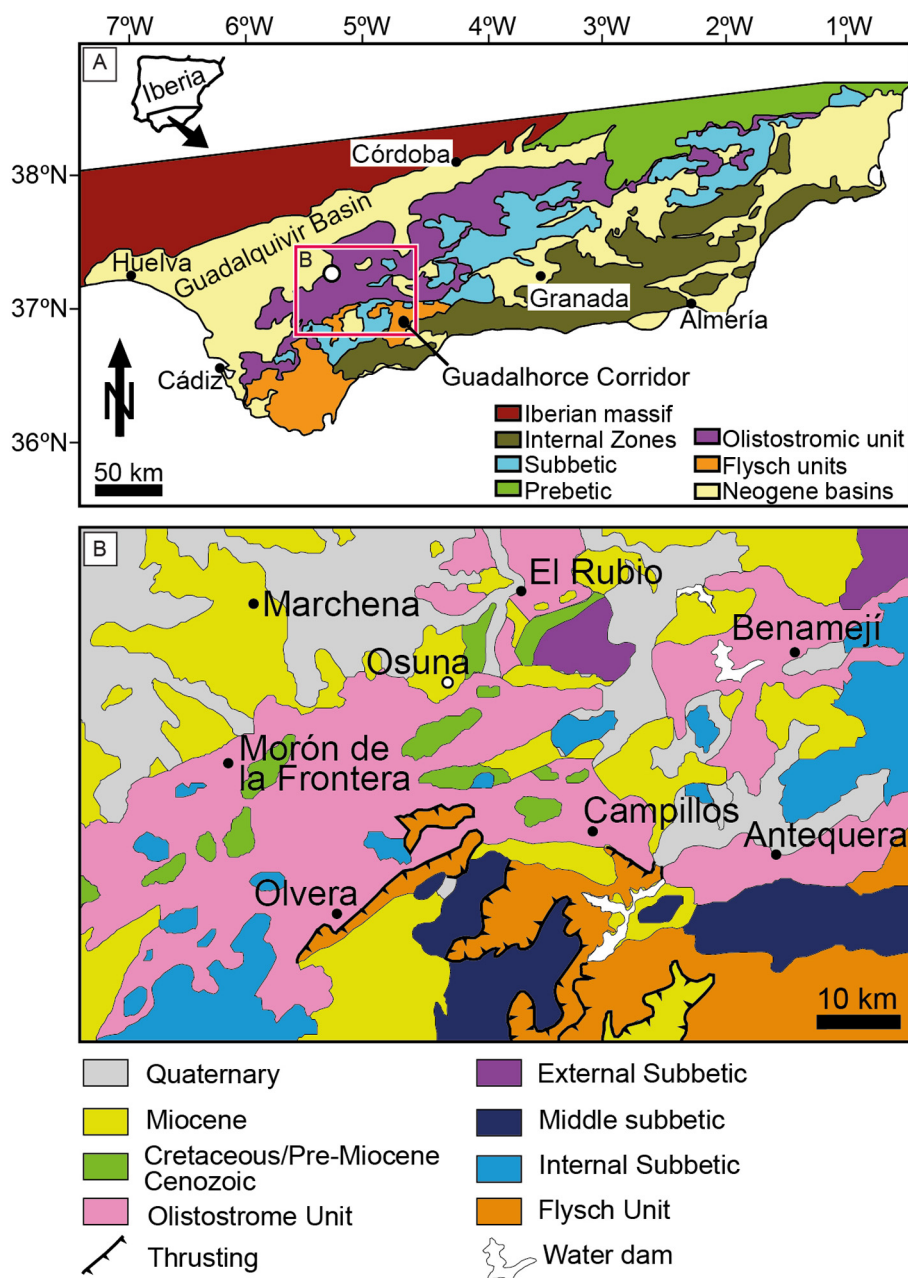
Fig. 1. Geological setting. A) Location of the study area in South Spain. Red frame indicates the position of panel B as well as the location of the Guadalhorce Corridor and the Osuna Quarry section (white dot). B) Close up of the different geological units cropping out in the surroundings of Osuna (37° 14′ N, 5° 06′ W).

the Iberian Peninsula, the Betic corridors, and in the northern part of Morocco, the Rifian corridors (Martín et al., 2001, 2009, 2014; Flecker et al., 2015; Capella et al., 2018; Krijgsman et al., 2018; Ng et al., 2021). The water exchange between the Mediterranean and the Atlantic during the early Messinian was characterised by AIW inflow through the Rifian corridors and MOW outflow through the Guadalhorce Corridor (Benson et al., 1991; Pérez-Asensio et al., 2012; Flecker et al., 2015; Krijgsman et al., 2018). This circulation pattern for the Atlantic-Mediterranean water exchange during the Miocene was named by Benson et al. (1991) "the siphon model", and that has been the paradigm up to date.

3. Methodology

In the study area, the mixed carbonate-siliciclastic deposits are exposed in the vertical walls of the quarry front. This allows for three-dimensional (3-D) observations in the field and on photogrammetric

models, but precludes detailed logging of stratigraphic sections. Drone images were used to obtain a complete view of the whole outcrop, as well as to observe stratigraphic sections and correlate them (Fig. 2A). Images were integrated into a 3-D photogrammetric model that was later studied using CloudCompare V2 (CloudCompare, 2021) and Virtual Reality Geological Studio (VRGeoscience Limited version 2.66.0.0) in order to estimate dip angle and direction, and thickness of the sedimentary bodies. The Osuna Quarry was also lithologically described and sampled in the accessible areas.

Foraminiferal assemblages from the size fraction >125 μm were studied in two silt beds, OSU-1 and OSU-M2 (Fig. 2B; Table 1). Planktonic foraminifera were studied to ascertain the age of the deposits, and benthic assemblages were used to infer the palaeoenvironmental conditions. The diversity and microhabitat preferences of the benthic foraminiferal assemblages were analysed. The relative abundance of elevated epibenthic species, which are suspension feeders, was calculated
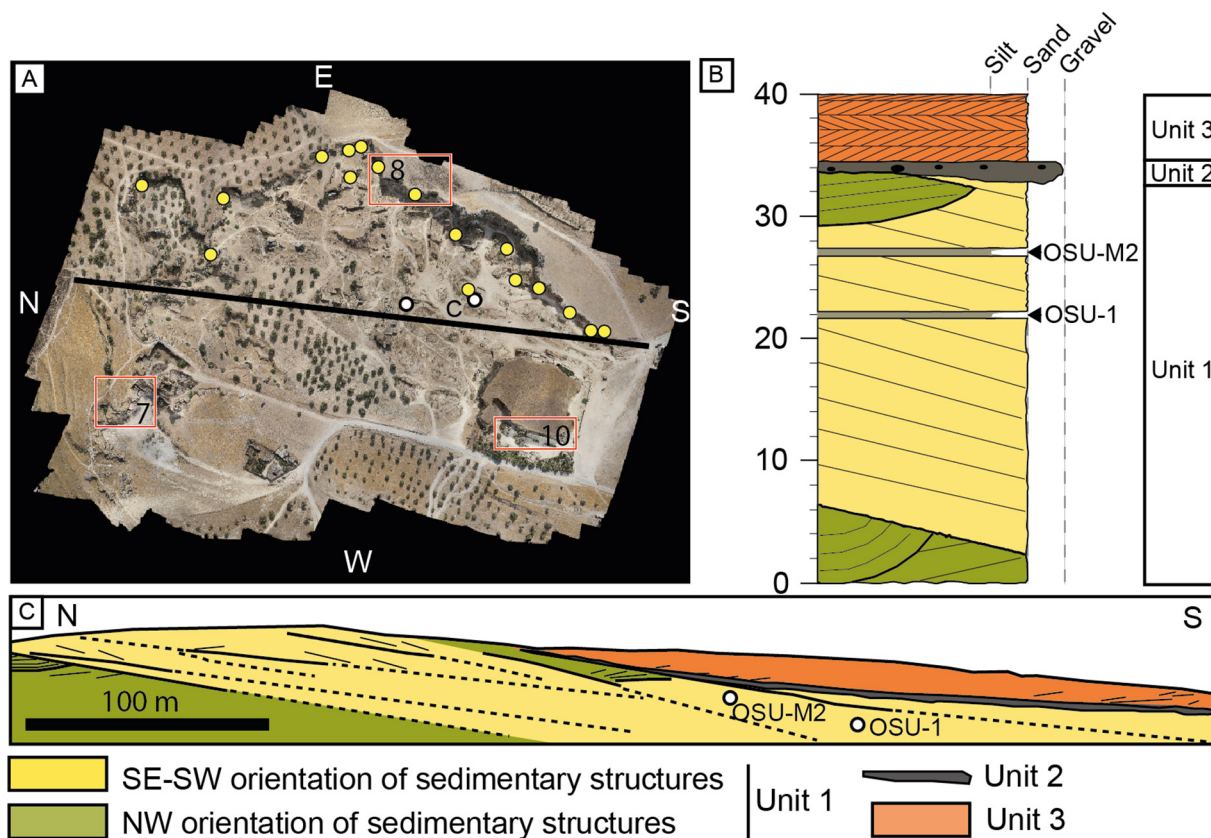
Fig. 2. Osuna Quarry. A) Top view of the photogrammetric model. Red frames indicate the position of the areas shown in Figs. 5, 6 and 7. Yellow dots indicate the position of the samples for sedimentological analysis. White dots indicate the position of the samples for micropalaeontological analysis. B) Stratigraphic profile of the Osuna Quarry section with the location of the micropalaeontology samples. C) Cross-section of the Osuna Quarry showing the geometry of the different units and the orientation of the sedimentary structures. Solid thick lines represent surfaces separating large sediment bodies traced on the photogrammetric model. Dashed lines are the likely continuation of those surfaces. Thinner lines represent the internal structures inside the sediment bodies. White dots indicate the position of micropalaeontology samples.

Table 1

Benthic foraminiferal assemblages of the studied samples showing the relative abundance (%) of each species (numbers in brackets). The assemblage water-depth range (AWDR), estimated water depth (EWD) (95 % confidence intervals in brackets), the planktonic/benthic ratio (P/B), percentage of transported shelf taxa, number of taxa (S), Shannon-Wiener index (H), dominance (D), and the percentage of infauna, epifauna and elevated epibenthic species are also indicated.

OSU-1	OSU-M2
Planulina ariminensis (**11.2**)	*Cibicidoides wuellerstorfi* (**18.8**)
Cibicidoides wuellerstorfi (10.8)	*Cibicidoides mundulus* (16.2)
Melonis pompilioides (9.2)	*Cibicides refulgens* (11.6)
Globocassidulina subglobosa (7.6)	*Planulina ariminensis* (7.9)
Siphonina reticulata (7.2)	*Globocassidulina subglobosa* (7.9)
Cibicidoides mundulus (5.6)	*Cibicides* sp. (7.9)
Cibicides refulgens (5.2)	*Cibicidoides* sp. (6.1)
Cibicides sp. (4.4)	*Melonis pompilioides* (4.3)
Cibicidoides sp. (4.4)	*Nodosaria* sp. (3.2)
Pullenia bulloides (3.2)	*Lobatula lobatula* (3.2)
Siphonodosaria lepidula (3.2)	
AWDR (m): 200–1000	AWDR (m): 200–1000
EWD (m): 427 (307–547)	EWD (m): 306 (218–394)
P/B ratio (%): 38.1	P/B ratio (%): 35.9
Transported shelf taxa (%): 18.2	Transported shelf taxa (%): 12.1
S: 31	S: 27
H: 3.0	H: 2.6
D: 11.2	D: 18.8
Infauna (%): 29.1	Infauna (%): 14.1
Epifauna (%): 70.9	Epifauna (%): 85.9
Elevated epibenthic species (%): 41.0	Elevated epibenthic species (%): 41.5

as a proxy for bottom currents (Lutze and Thiel, 1989; Schönfeld, 1997, 2002a, 2002b; García-Gallardo et al., 2017). The assemblage water-depth range (AWDR) was established by overlapping the water-depth ranges of all species from the benthic foraminiferal assemblages. The estimated water depth (EWD) is based on a quantitative palaeobathymetry calculation using the approach of Pérez-Asensio (2021), which consists of removing abundant infaunal benthic foraminifera prior to applying a transfer equation based on benthic foraminiferal water-depth ranges and presence/absence of species. Furthermore, the percentage of transported shelf taxa and the planktonic/benthic ratio (P/B ratio hereafter) were calculated to infer downslope transport and palaeo-water depth, respectively (van der Zwaan et al., 1990; Murray, 1991, 2006). Additionally, twenty rock samples were taken for microfacies analysis on thin sections.

4. Results

4.1. Sedimentary succession

The studied section at the Osuna Quarry comprises a 40-m thick mixed carbonate-siliciclastic succession (Fig. 2B) that can be subdivided into three units according to the facies (Fig. 3) as well as the type and orientation of the sedimentary structures (Figs. 2C, 4, 5).

4.1.1. Unit 1

The exposed part of this unit is 33-m thick from the base of the quarry to the base of the conglomerate body of Unit 2 (Fig. 2B). The
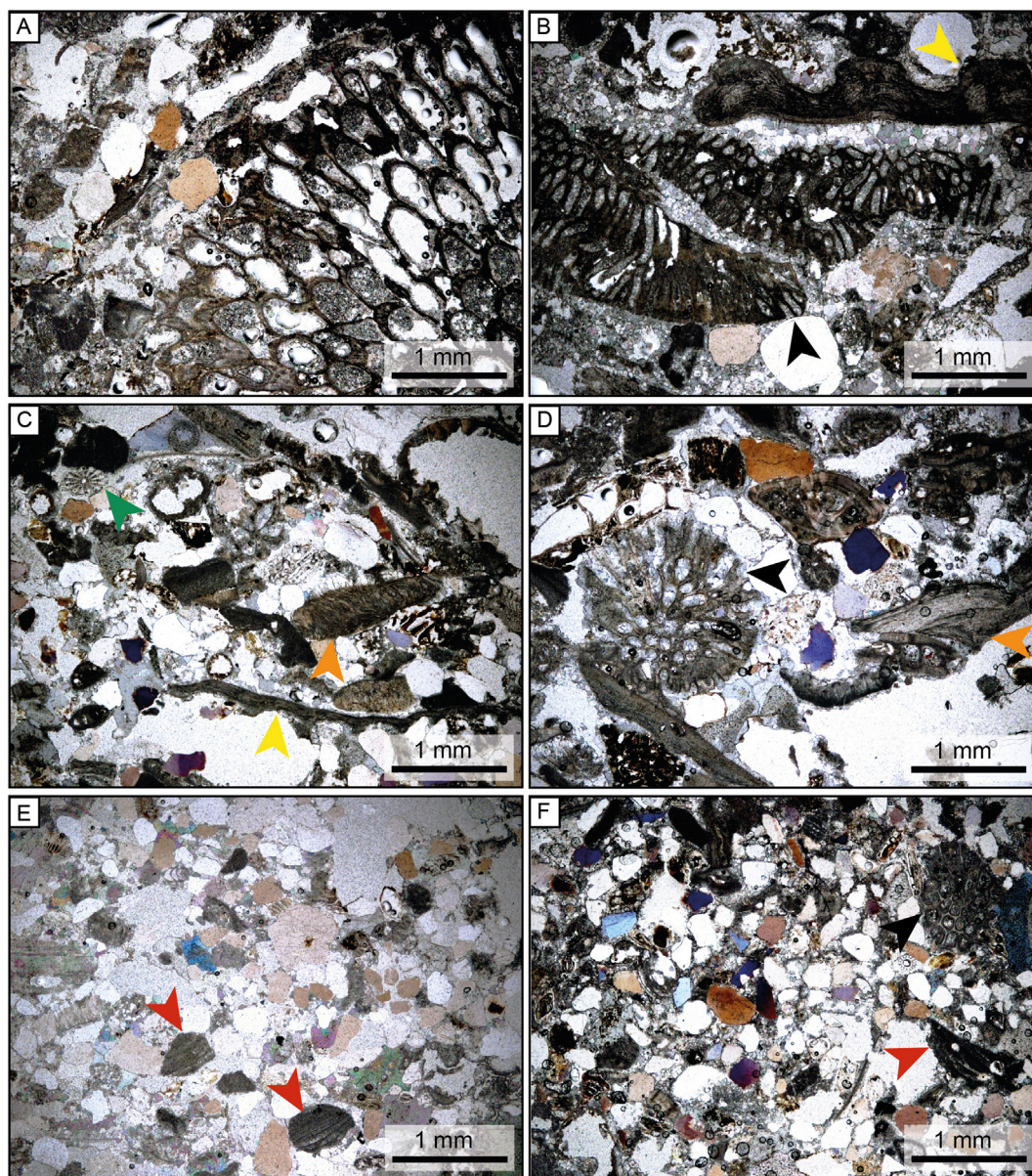
Fig. 3. Microfacies of the Osuna Quarry. A) Bryozoan nodule surrounded by siliciclastic grains from a Unit 1 rudstone interval. B) Bryozoan (black arrow) and bivalve (yellow arrow) fragments in a mixed carbonate-siliciclastic matrix from a Unit 1 rudstone interval. C) Echinoid spine (green arrow), oyster fragment (orange arrow) and swimming bivalve shell (yellow arrow) in a dominantly siliciclastic matrix from a Unit 1 packstone interval. D) Bryozoan nodule (black arrow) and oyster remain (orange arrow) from a Unit 1 packstone interval. E) Red algae nodules (red arrow) in a siliciclastic sand from Unit 3. F) Bryozoan (black arrow) and red algal (red arrow) fragments and abundant siliciclastic grains in a fine carbonate matrix from a Unit 3 packstone.

unit consists of a succession of 9 to 10 large sediment bodies, from 5 to 10 m in thickness and few hundred metres of lateral extension (Fig. 2C). The facies composition is very uniform, consisting mostly of bryozoan nodules, echinoid and mollusc fragments (Fig. 3A–C). Siliciclastics, mostly quartz, are common and range between a 15 % and a 60 % (Fig. 3C). All the bioclasts present evidence of mechanical abrasion, such as rounding and smoothing of surface features. Coralline red algal and oyster fragments can be locally up to 50 % of components (Fig. 3). Intraclasts are present in some intervals. Carbonate lithofacies ranges between rudstone (Fig. 3A, B) and packstone (Fig. 3C, D). Packstone beds are usually lighter in colour than rudstone ones (Fig. 4A). The contacts between packstone and rudstone are usually sharp (Fig. 4A). The rudstone beds are poorly sorted and contain siliciclastic grains up to 3 cm in size (Fig. 4B), and large bivalve fragments and rhodoliths both up to 4 cm in diameter. Bryozoan nodules in these beds can be up to 3 cm in size, but most bioclasts are usually around 1 cm. Packstone beds have better sorting (Fig. 4C) and exhibit better-

developed cross-bedding (Fig. 4D). In any case, cross-bedding is common in both facies (Fig. 6). At around 22 m and 27 m from the base of the section there are two 10-cm thick fine-grained beds consisting of silt with a few dispersed, small bioclasts (Fig. 4E, F). These are the beds sampled for the analyses of planktonic foraminiferal biostratigraphy and benthic foraminiferal assemblages (Table 1).

Since the facies are very homogenous, sediment bodies within the unit are distinguished based on the displayed structures. Most bodies consist of planar cross-beds ranging in thickness from 20 to 100 cm and dipping between 5 and 10° to the S, mostly to the SE and less commonly to the SW (Fig. 5). Most of these strata display internal cross-bedding and cross-lamination also dominantly oriented to the SE (Fig. 4D) with minor structures apparently dipping to west to northwest (Fig. 6). There are two bodies, one at the bottom and another in the upper part of the unit (Fig. 2B, C), with different geometry and sedimentary structures, which are oriented to the west to northwest (Fig. 2C). The 6-m thick basal body is well stratified with concave-up foresets
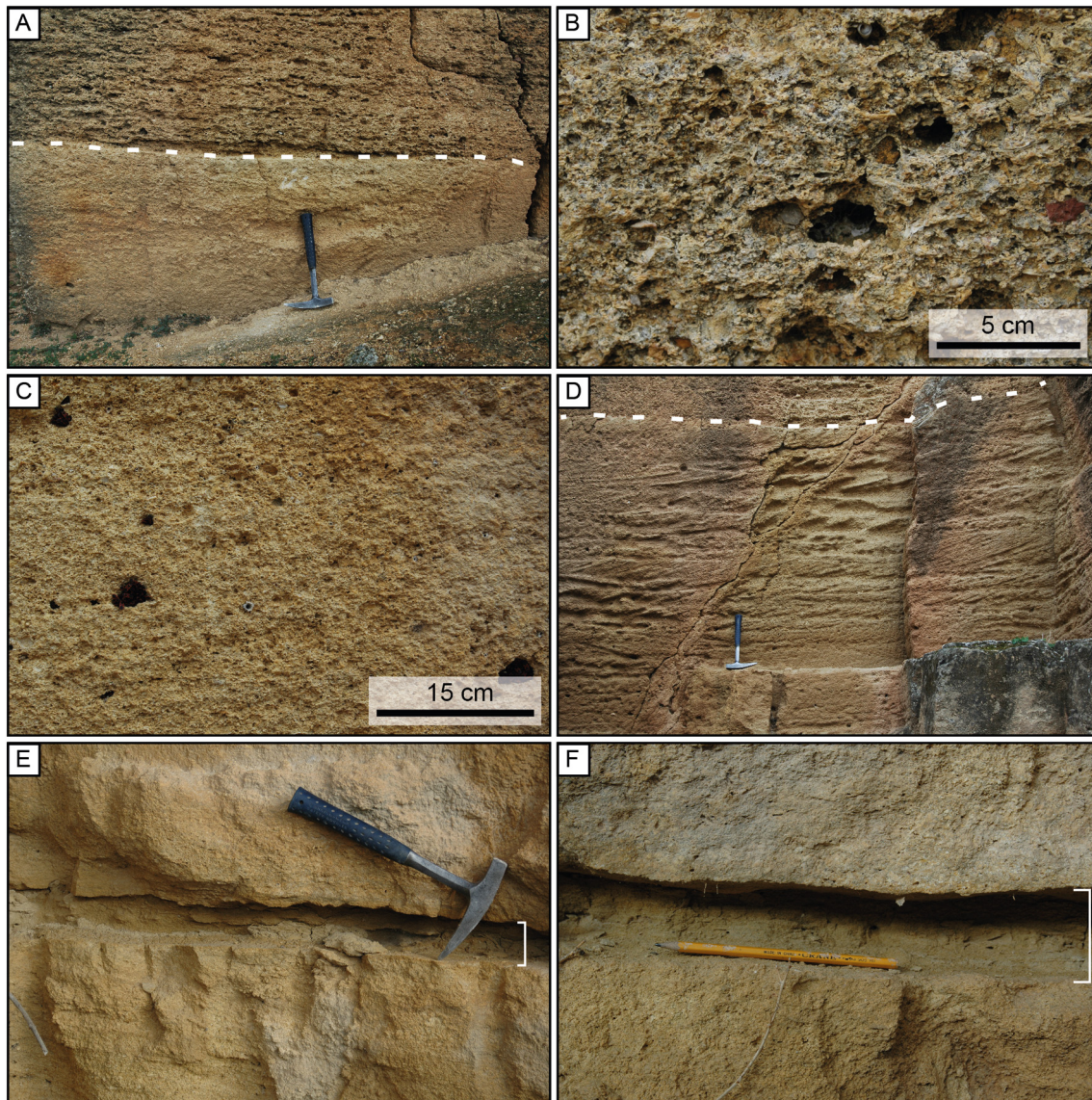
Fig. 4. Facies of the Osuna Quarry. A) Reactivation surface (white dashed line) separating well-sorted packstone and overlying coarser-grained rudstone in Unit 1. East to the right. Hammer is 33-cm long. B) Close-up of rudstone facies with abundant siliciclastic clasts from Unit 1. C) Close-up of packstone facies from Unit 1. Note the homogeneity of this facies in contrast with rudstone. D) Outcrop photograph of centimetre-scale cross-bedding in packstone from Unit 1. The white dashed line represents a reactivation surface marking a change in grain size. East to the left. E) Outcrop photograph of a fine-grained bed (white bracket) intercalated in packstone facies of Unit 1. F) Detail of the fine-grained bed (white bracket) intercalated in packstone facies of Unit 1 where sample OSU-1 was taken.

around 40-cm thick, which laterally pinch out to the north (Fig. 7). The foresets have a minimum of 5° and a maximum inclination of ~15°. These foresets are erosively cut off at their top by the lowest sediment body dipping to the SE (Fig. 7). The 4-m thick body at the top of the unit with sedimentary structures oriented to the N (Fig. 2B, C) displays planar cross-bedding between 15 and 30 cm in thickness (Fig. 8). The top of this body is erosively cut by the uppermost south-dipping body and both are cut by the base of the overlying unit (Fig. 8).

4.1.2. Unit 2

This unit is made up of a 0.5 to 2-m thick conglomerate body that spreads laterally for nearly 200 m and thins out northwards (Fig. 2B, C). Locally, it exhibits a poorly developed internal bedding with beds around 0.5-m thick. In its northern part, the conglomerate dips around 5° to the S (203° SE) and becomes subhorizontal to the southern end of the outcrop following the morphology of the top of Unit 1 (Fig. 2). The erosive base of the conglomerate is irregular (Fig. 9A, B). This facies consists of terrigenous clasts ranging in size from 2 to 5 cm, floating in a coarse-grained mixed

siliciclastic-bioclastic sand. The clasts are mostly reddish sandstones and quartzites and are relatively well-rounded. Some clasts are encrusted by bryozoans and/or show *Gastrochaenolites* sp. borings (Fig. 9C).

4.1.3. Unit 3

The uppermost unit is around 6-m thick and extends laterally for >200 m (Fig. 2B, C). Individual beds range between 0.5 and 1 m in thickness (Fig. 10). These beds are almost subhorizontal (Fig. 10). This unit consists of a well-sorted, predominantly siliciclastic (~60 %) fine sand made up mainly of quartz and feldspar grains with some bioclastic components, mainly bryozoan and echinoid remains (Fig. 3E, F). Where the carbonate fraction is higher, coralline red-algal nodules and bivalve fragments are common. Larger benthic foraminifera such as Nummulitidae and *Amphistegina*, are also present.

This unit is characterised by the occurrence of herringbone structures (Fig. 10). The beds show internal cross-stratification dipping between 4° and 17°, mainly oriented towards 325° NE (Fig. 5). There is a subordinate cross-bedding component dipping towards 184° S (Fig. 5).
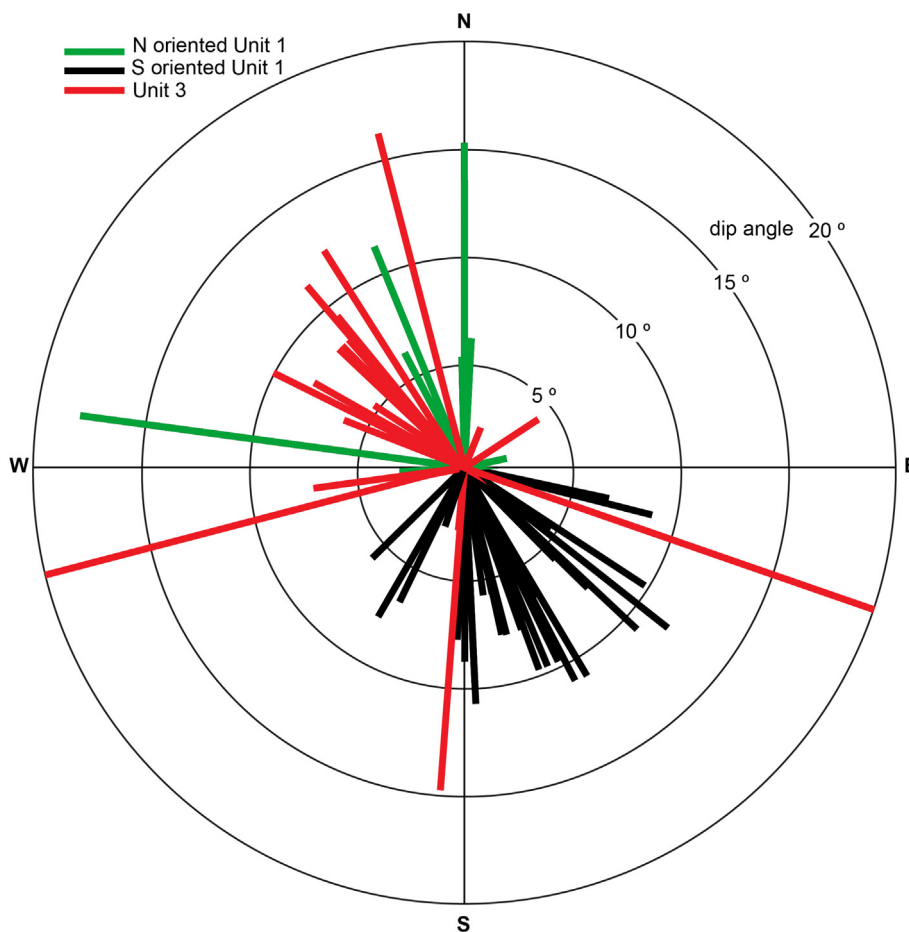
Fig. 5. Orientation of sedimentary structures (67 measurements).

4.2. Planktonic foraminiferal assemblages

Benthic foraminifera dominate the two samples collected in the Osuna Quarry, while planktonic ones are scarce and taphonomically distorted, thus precluding quantitative analysis of their relative abundance. Planktonic foraminiferal assemblages are characterised by *Neogloboquadrina acostaensis*, *N. humerosa*, *Globorotalia scitula*, *G. miotumida* group, *Turborotalita quinqueloba*, *Globigerinoides extremus*, *G. bulloideus*, *G.* cf. *conglobatus*, and *Sphaeroidinellopsis* sp. Among keeled globorotaliids, we found only a few specimens of *G. miotumida*

(*Globorotalia dallii*). *Globigerinoides bulloideus* ranges from the base of the Messinian to the top of the Zanclean (early Pliocene) (Kennett and Srinivasan, 1983; BouDagher-Fadel, 2015), suggesting that the Osuna deposits can likely be assigned to the Messinian.

4.3. Benthic foraminiferal assemblages

The benthic foraminiferal assemblage from sample OSU-1 (Fig. 2B) is dominated by *Planulina ariminensis* (Table 1). The most abundant additional taxa are *Cibicidoides wuellerstorfi*, *Melonis pompilioides*,
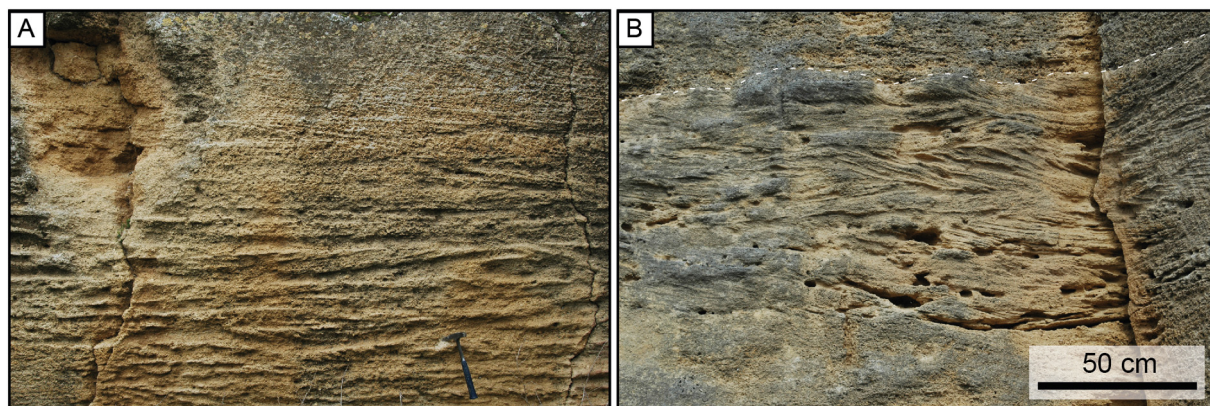
Fig. 6. Small-scale structures of Unit 1. Oscillation ripples of diverse orientation in A) rudstone and B) packstone intervals. The white dashed line represents a reactivation surface marking a change in grain size. North is located to the left in both pictures.
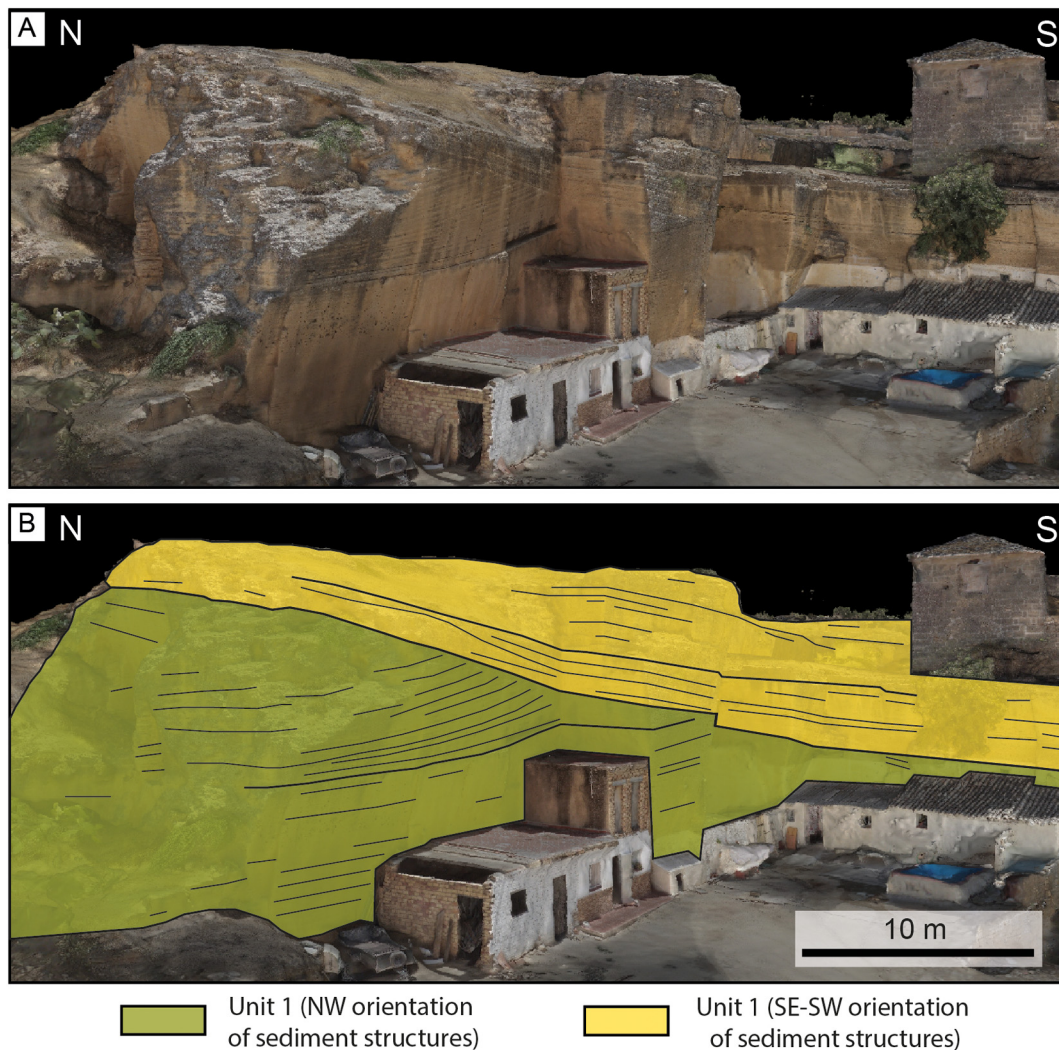
Fig. 7. Bottom part of Unit 1. A) Three-dimensional photogrammetric model and B) interpretation of the sediment bodies and their internal structure.

Globocassidulina subglobosa, *Siphonina reticulata*, *Cibicidoides mundulus* and *Cibicides refulgens* (Table 1). The assemblage water-depth range (AWDR) extends from 200 to 1000 m. The estimated water depth (EWD) gives a more precise palaeo-water depth of around 450 m with an uncertainty from 300 to 550 m (Table 1). The P/B ratio (38.1 %) and percentage of transported shelf taxa (18.2 %) are low. Diversity is high according to high S and H and low D values (Table 1). Infaunal taxa are less abundant (29.1 %) than epifaunal ones (70.9 %). Among the latter, elevated epibenthic species represent 41 % of the assemblage.

In the sample OSU-M2 (Fig. 2B), the benthic foraminiferal assemblage is dominated by *Cibicidoides wuellerstorfi*, with *Cibicidoides mundulus*, *Cibicides refulgens*, *Planulina ariminensis*, *Globocassidulina subglobosa*, *Cibicides* sp. and *Cibicidoides* sp. as most abundant secondary taxa (Table 1). The AWDR extends from 200 to 1000 m, similarly to sample OSU-1. However, the EWD is lower than in sample OSU-1, with a value of around 300 m and uncertainty from 200 to 400 m (Table 1). The P/B ratio and percentage of transported shelf taxa show low values of 35.9 and 12.1 %, respectively. Diversity is high, but slightly lower than in sample OSU-1 as suggested by lower S and H, and higher D. The assemblage is dominated by epifauna, showing less infaunal taxa than sample OSU-1. Elevated epibenthic species relative abundance (41.5 %) is very similar to that of sample OSU-1 (Table 1).

5. Discussion

5.1. Depositional environment

The three units described herein are the result of different sedimentary processes. Persistent bottom currents, fluvial discharge and tides are the main processes shaping the Osuna Quarry section.

5.1.1. Large sedimentary structures and bottom currents

The first sedimentary body at the base of Unit 1 displays metre-scale concave-up foresets that can be interpreted as the internal structure of migrating dunes (Fig. 7). The sediment grain size and height of the foresets suggest that the migrating dunes that formed this body was deposited by a current flowing towards the northwest at a speed ranging from 40 to 200 cm/s using the bedform classification of Rebesco et al. (2014). The truncation of the foreset tops of this body is distinctive of contourite drift deposits in which changes in the intensity or flow direction of the bottom current result in such reactivation surfaces (Shanmugam, 2008, 2017; Rebesco et al., 2014). The truncation of the lowermost body of Unit 1 is related to the change of flow direction to the SE (Figs. 2, 7). Similar large-scale sedimentary structures were reported in siliciclastic drifts from the coeval Rifian Corridor in Morocco (Capella et al., 2018).
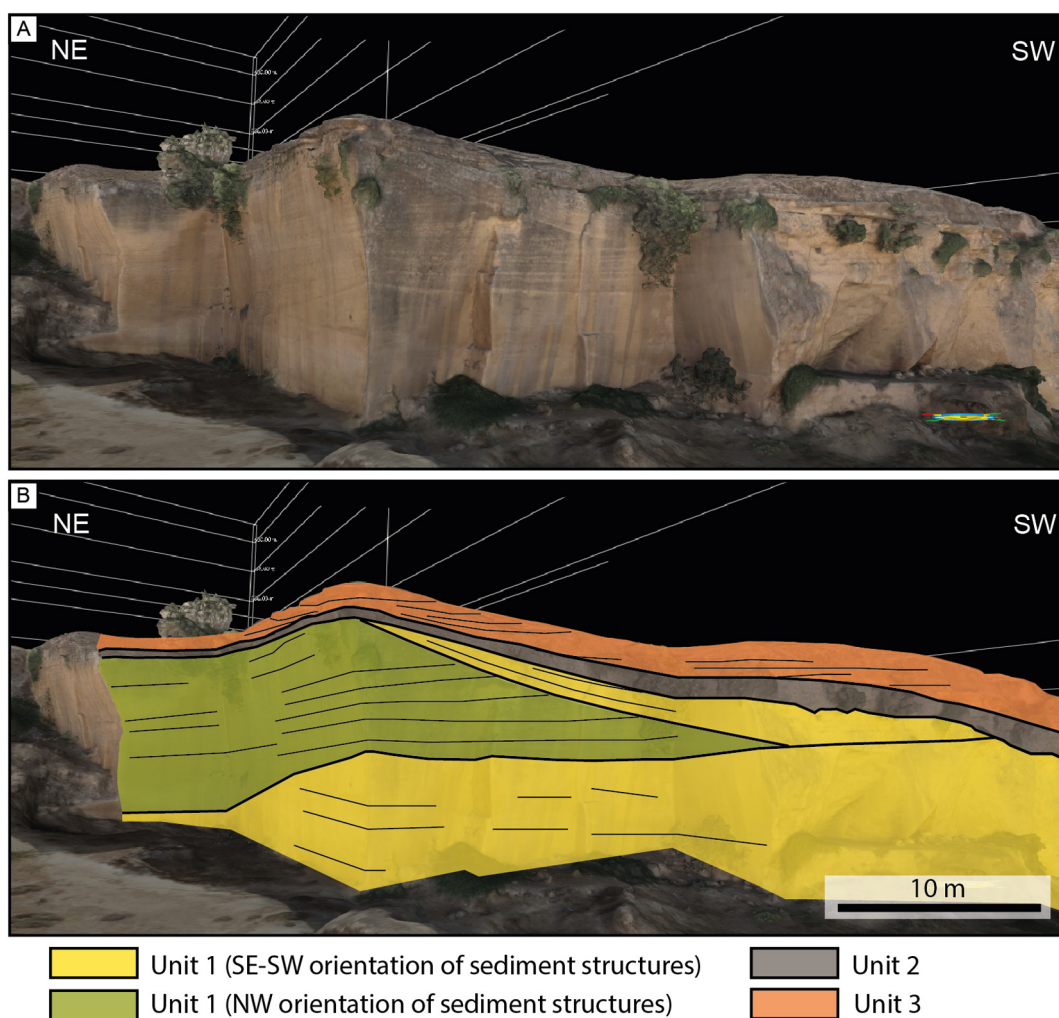
Fig. 8. Topmost part of Unit 1, Unit 2, and Unit 3. A) Three-dimensional photogrammetric model and B) interpretation of the sediment bodies and their internal structure.

Currents flowing to the S were dominant during deposition of Unit 1 (Fig. 4). Besides the dominant large-scale structures, there are small-scale bedforms with diverse orientations (Fig. 6), that can be interpreted as oscillation ripples formed on the surface of larger dunes migrating to the south Similar structures were reported from outcrops related to equivalent settings in Pleistocene straits (Longhitano et al., 2014). Within this stratigraphic interval with southeast to southwest-oriented structures (Figs. 7, 8), there are facies changes that can be interpreted as changes in bottom current speed (Fig. 4A). The sharp contacts between well-sorted packstone and overlying poorly sorted rudstone beds (Fig. 4A) can be interpreted as reactivation surfaces representing an acceleration of currents, which necessarily exceeded the speed of 200 cm/s in order to transport sediment larger than 2 mm (Shanmugam et al., 1993a, 1993b; Stow et al., 2009). Beds with abundant rhodoliths and larger siliciclastic grains (up to 3 cm) were the result of the fastest currents in the section. In contrast, the two silt beds record the slowest bottom currents in Unit 1, with an approximate speed between 10 and 40 cm/s (Stow et al., 2009). This current speed range is consistent with the percentage of elevated epibenthic species found in both silt beds, which indicates a near-bottom current speed of around 35 cm/s using the equation of Schönfeld (2002a), which is an exponential relationship between the relative abundance of elevated epibenthic foraminifera and current velocity. The flow direction of the bottom currents changed to north to northwest during a time interval in the upper part of Unit 1, returning again to a S direction before its end (Fig. 8).

A persistent bottom current at the northern entrance of the Guadalhorce Corridor is considered responsible for the formation of the Osuna Quarry sequence of Unit 1, dominantly dipping to the S (Fig. 2). The occurrence of large-scale traction structures, the presence of sharp contacts among facies interpreted as reactivation surfaces and the dominance of the main flow direction deduced from the sedimentary structures are diagnostic criteria for classifying the Unit 1 of the Osuna Quarry as a contourite drift (Shanmugam et al., 1993a, 1993b). The bottom currents were persistent in time according to the dominance of unidirectional structures, either flowing to the north at the bottom and top of the sequence or flowing to the S in the rest of the succession.

5.1.2. Composition and texture of the sediment

The degree of fragmentation and abrasion of the allochems is consistent with the action of strong bottom currents (Martín-Chivelet et al., 2003, 2008; Longhitano et al., 2014; Rebesco et al., 2014; Lüdmann et al., 2018; Eberli and Betzler, 2019; Reolid et al., 2019; Longhitano and Chiarella, 2020). The bioclastic fraction of the facies with abundant bryozoans, echinoids, molluscs, and red algae is a typical Miocene bryomol assemblage (Nelson, 1988). Estimated water depths based on benthic foraminiferal assemblages from the two silt beds within Unit 1 suggest a deep environment with palaeo-water depths ranging from around 220 to 550 m (Table 1). The abundance of the deep-water species *C. wuellerstorfi* and *C. mundulus* supports this water depth range (van Morkhoven et al., 1986; Holbourn et al., 2013; Pérez-Asensio et al., 2017). Preferential destruction of less-resistant planktonic
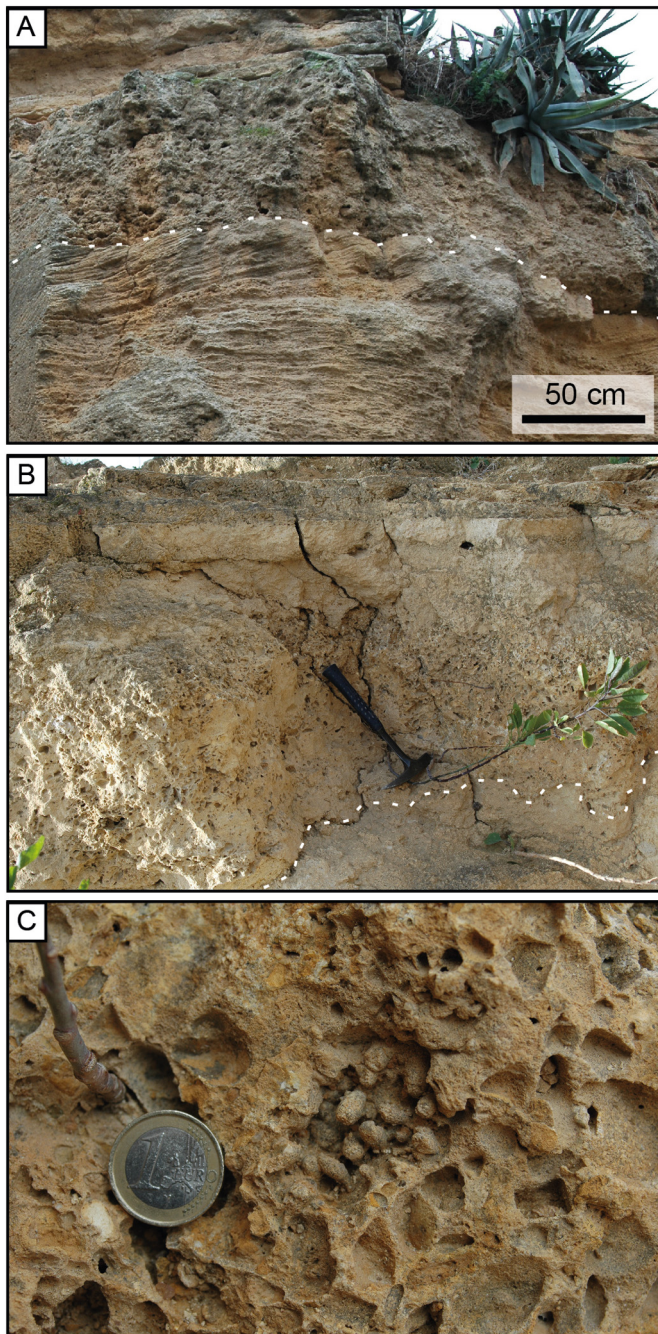
Fig. 9. Unit 2. A) Conglomerate body of Unit 2 overlying the packstone facies of the top of Unit1. The white dashed line represents the erosional base of the conglomerate. B) Close-up of the conglomerate body of Unit 2 and overlying packstone of Unit 3 (darker sediment). Hammer is 33-cm long. C) Close-up view of the borings (preserved as a counter mould in the image) present in some clasts of the conglomerate.

foraminiferal shells by the action of energetic bottom currents might explain the anomalously low P/B ratio values (Table 1), which are much lower than values recorded in deep settings (van der Zwaan et al., 1990; Murray, 1991, 2006). Speeds of 25–30 cm/s are the minimum required for moving rhodoliths (Marrack, 1999), but higher speeds of at least 80 cm/s are needed to initiate the movement of rhodoliths around 5 cm in size (Harris et al., 1996). These current-speed values are consistent with the values inferred from the epibenthic percentage in the benthic foraminifera assemblage (Table 1). The grain size of some of the bioclasts of the Osuna Drift, especially rhodoliths and some bryozoan nodules (up to 3–4 cm), suggests that the source area should not be

far from the place of final deposition, since it is difficult for bottom currents alone, without the combined action of turbidity currents, to transport such coarse grains for long distances (Lima et al., 2007; Coletti et al., 2015; Bassi et al., 2017).

With respect to the siliciclastics, their composition with abundant quartz and feldspar as well as sandstone lithoclasts indicates that the most likely source area was to the south, where Triassic materials crop out (Verdenius, 1970; Cruz-Sanjulián, 1975; Divar and Cruz-Sanjulián, 1986). The Guadalquivir Olistotrome Units formed the main emergent areas at the time of deposition of Unit 1 (Fig. 1). The Triassic rocks involved in the large blocks of the GOU are sandstone, clay, and gypsum typical of the Keuper facies (Divar and Cruz-Sanjulián, 1986). The erosion of these rocks provided terrigenous material that reached the coast by alluvial discharge and was later redistributed in the basin by bottom currents. The conglomerate body of Unit 2 represents an event of intense alluvial input in a relatively nearshore shallow environment, likely related to uplift of the southern margin of the Guadalquivir Basin. This is consistent with the size of clasts and the presence of *Gastrochaenolites*. The uplift hypothesis fits with the regional tectonic regime of the Betic Cordillera during the late Miocene (López-Garrido and Sanz de Galdeano, 1999; Galindo-Zaldívar et al., 2019) and explains the abrupt change from a relatively deep palaeoenvironment controlled by bottom currents, Unit 1, to a shallow one, Unit 2 and Unit 3.

5.1.3. Tide controlled sedimentation

Unit 3 displays two sets of cross-bedding with different directions, a dominant dipping to the northwest and a subordinate to the S (Figs. 5, 10). Despite the dominant northward stratification (Fig. 10), the alternation of cross-bedding with two orientations results in a characteristic herringbone structure typical of environments dominated by tides (Davis, 2012). The contacts separating successive beds with internal structures migrating to the northwest are interpreted as reactivation surfaces, also indicative of tidal influence (Klein, 1970; Davis, 2012). These reactivation surfaces separate bedsets with different orientation of the sediment structures and the same facies, in contrast with the reactivation surfaces in the drift unit (Unit 1, Fig. 4A) where grain size significantly changes at the surface. The grain-size variation at the reactivation surfaces in Unit 1 resulted from intensification of the bottom currents in contrast with the tidal origin of the reactivation surfaces in Unit 3. The latter surfaces were generated because the subordinate current, the one flowing to the southeast, was not always strong enough to reverse the direction of migrating foresets, but it eroded the sediment of the upper part of the previous bed producing an erosional surface (Davis, 2012). The prevalent action of currents flowing to the northwest resulted in the stacking of 0.5–1-m thick beds with cross-stratification pointing in that direction (Fig. 10). Only during periods of enhanced tidal currents flowing towards the S, cross-bedding pointing towards the southeast developed.

5.2. Palaeogeography and palaeoceanography

Carbonate drifts with fossil assemblages and grain sizes similar to those of the Osuna Drift are relatively rare (Viana, 2001; Lüdmann et al., 2018; Eberli et al., 2019; Reolid et al., 2019; Reolid and Betzler, 2019), in comparison with their fine-grained counterparts (Stow et al., 1998, 2002; Huneke and Stow, 2008; Betzler et al., 2014; Rebesco et al., 2014; Bunzel et al., 2017; Reolid and Betzler, 2019; Reolid et al., 2021; Stow and Smillie, 2020; Hüneke et al., 2020). Contourite drift deposits with coarse-grained concentrations develop in response to high-velocity bottom-current activity in shallow straits, narrow contourite moats, and passageways (Rebesco et al., 2014; Longhitano et al., 2014; Lüdmann et al., 2018; Eberli and Betzler, 2019; Eberli et al., 2019; Reolid et al., 2019). We propose that the Osuna Drift formed at the northern entrance of the Guadalhorce Corridor that connected the Atlantic Ocean and the
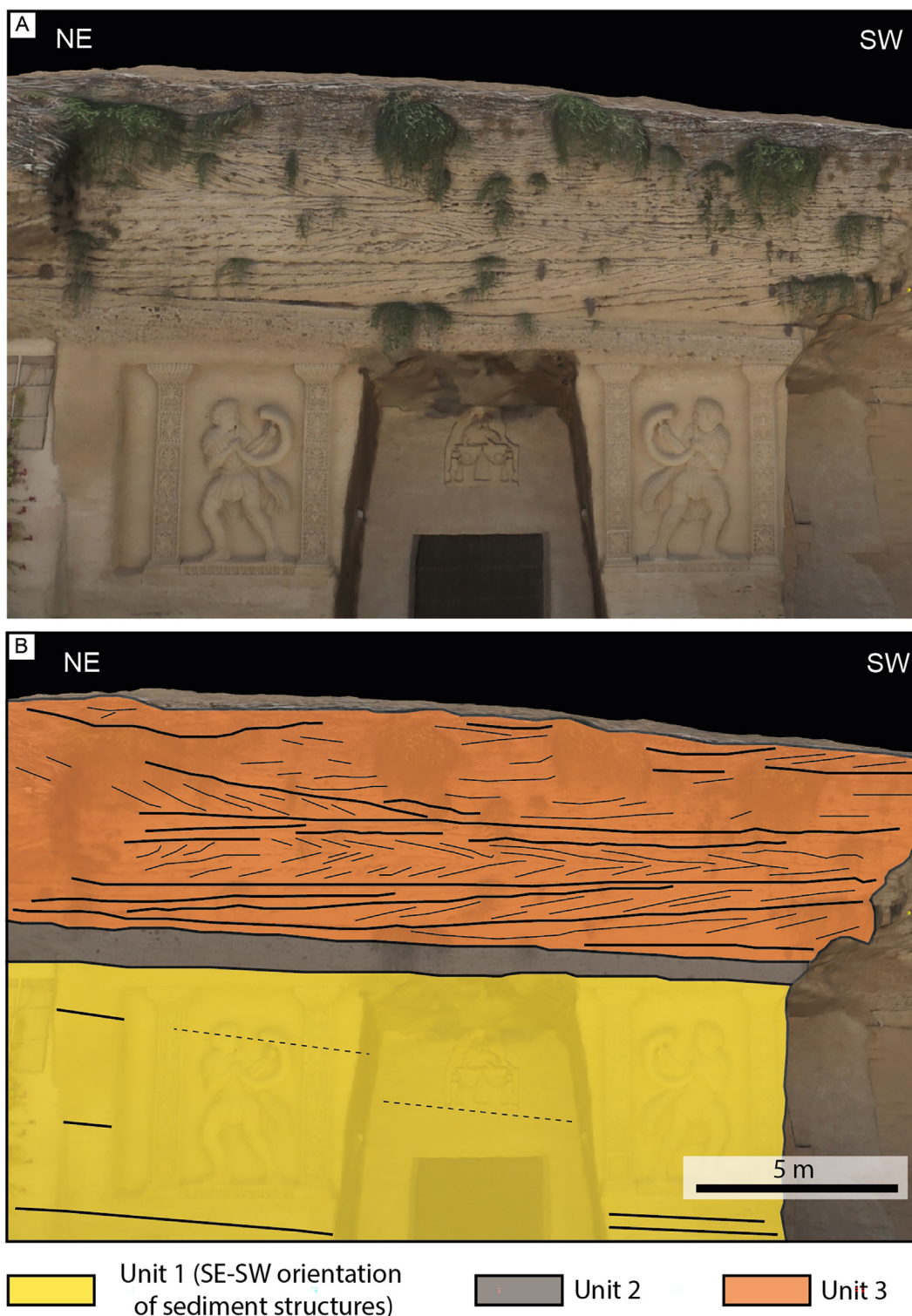
Fig. 10. Detail of the sedimentary structures of Unit 3. A) Three-dimensional photogrammetric model and B) interpretation of the sediment bodies and their internal structure. Thick lines in Unit 3 represent reactivation surfaces separating beds containing sedimentary structures with the same orientation.

Mediterranean Sea during the Late Miocene (Martín et al., 2001, 2014). The location of the Osuna Quarry, approximately 30 km to the northwest of the northernmost outcrop of the Guadalhorce Corridor (Figs. 1, 11A), and the age of the studied section are consistent with this interpretation.

The northwest sedimentary structures recorded in the Guadalhorce Corridor are unidirectionally directed towards the northwest (Martín et al., 2001). This flow direction of the bottom currents is consistent

with the siphon model of Benson et al. (1991), suggesting that the water exchange between the Mediterranean and the Atlantic during the early Messinian was characterised by Atlantic inflow (AIW) through the Rifian Corridors and Mediterranean Outflow Water (MOW) through the Guadalhorce Corridor (Benson et al., 1991; Pérez-Asensio et al., 2012). However, the dominance of structures oriented towards the southeast in the Osuna Drift seems to contradict the siphon model of Benson et al. (1991). The occurrence of AIW through the Rifian
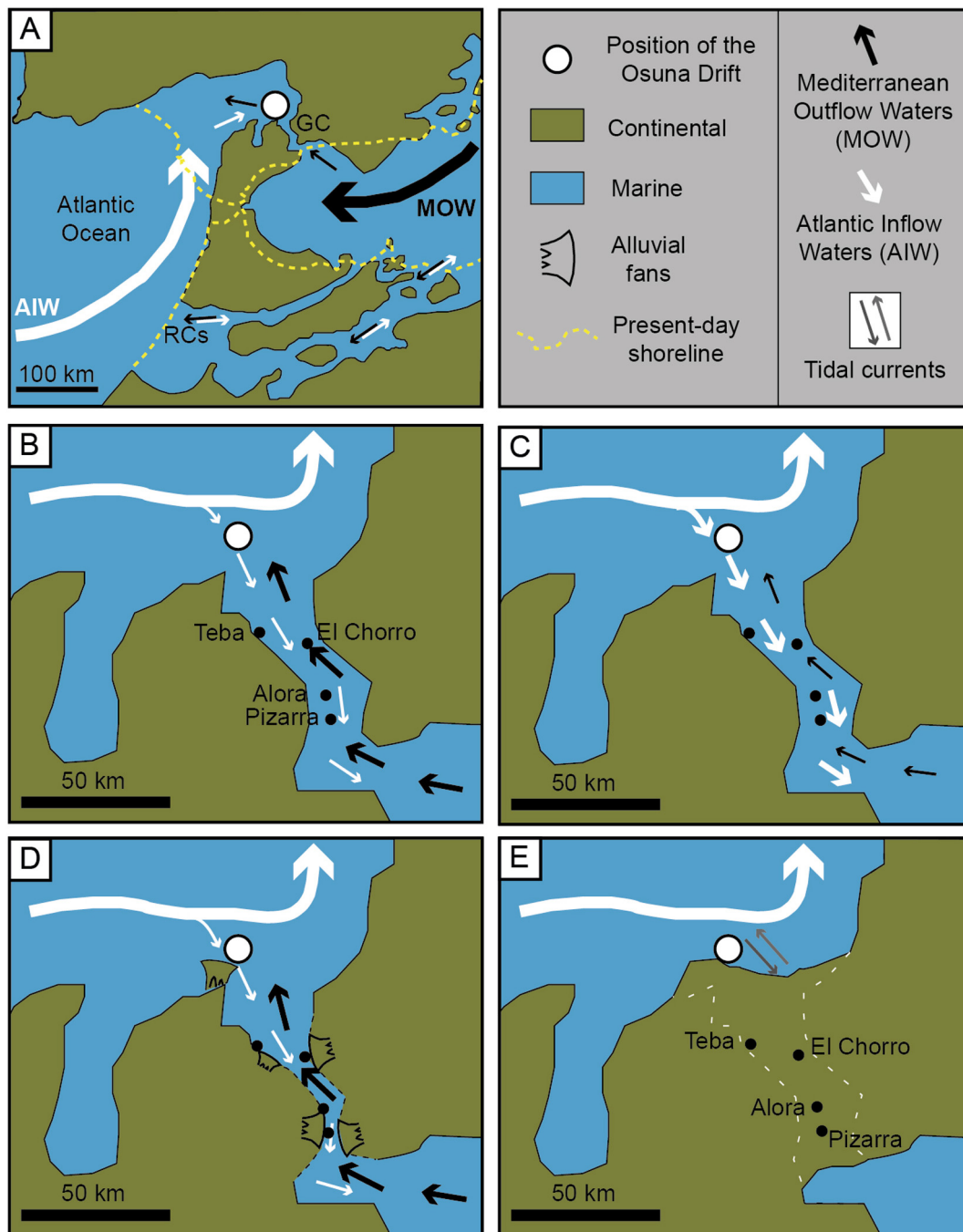
Fig. 11. Palaeogeography and palaeoceanography at the time of deposition of the Osuna Drift (latest Tortonian-earliest Messinian). A) Palaeogeographic reconstruction after Martín et al. (2009), including the main flow direction of the Atlantic and Mediterranean currents. GC: Guadalhorce Corridor; RCs: Rifian corridors. B) Close-up of the Guadalhorce Corridor and the Osuna area with the location of the main outcrops within the Guadalhorce Corridor (after Martín et al., 2001). The arrow thickness represents the proposed (see text) bottom current pattern during relative highstands with a dominance of the MOW that produced sedimentary structures directed towards the northwest in the Osuna Drift. RB: Ronda Basin. C) During relative sea-level lowstands, the AIW was dominant and sedimentary structures pointing to the southeast developed. D) Likely because of intense uplift, there was a widespread occurrence of alluvial fans inside the Guadalhorce Corridor (Martín et al., 2001). The general reconfiguration of the area resulted in a change in the style of deposition marked by the conglomerate body of Unit 2 in the Osuna Quarry. E) The tidal deposits of Unit 3 represent the sedimentation in the Osuna area after the closure of the Guadalhorce Corridor (white dashed line).

Corridors during the Miocene has been repeatedly reported (Fig. 11A; Flecker et al., 2015; Capella et al., 2018; Ng et al., 2021), but the Osuna Drift is the first evidence of Atlantic inflow through a Betic corridor during the Messinian.

At present, lower salinity waters from Atlantic (AIW) flow superficially eastward into the Mediterranean, and dense, saline intermediate and deep Mediterranean waters flow westward (MOW) promoting the occurrence of two drift systems related to both opposite bottom currents, inflow and outflow, in the area of the Strait of Gibraltar at different water depths (Hernandez-Molina et al., 2006; Hernández-Molina

et al., 2011, 2013, 2014; Ercilla et al., 2002). This can be an analogue for the opposite directions observed in the Osuna Drift and its coeval deposits in the Guadalhorce Corridor.

Hernández-Molina et al. (2014) already stated that relative sea-level fluctuations related to glaciations or regional tectonics during the Quaternary might result in variations in the intensity of the MOW and its expression in the sedimentary record. It was proposed that the MOW is weaker during lowstands (Nelson et al., 1999; Hernández-Molina et al., 2014). Relative sea-level changes, which were common and of significant amplitude during the Messinian

(Reolid et al., 2016b), together with the deepening of the interface between two water masses at the exit of a strait (Millot, 2014), can explain the different bottom current directions recorded in the Osuna Drift. During relative sea-level highstands, dense saline bottom waters flowed from the Messinian through the Guadalhorce Corridor and then descended until reaching the deeper environment at the exit of the strait, where bottom currents generated the northwest migrating dunes found at the bottom of the Osuna Quarry (Figs. 2, 7, 11B). When the sea level was relatively lower, at water depths from around 220 to 550 m of water depth (Table 1), the AIW currents were enhanced in the Osuna area resulting in sediment bodies migrating towards the southeast (Fig. 11C). This situation was later reverted during deposition of the upper body in Unit 1 with structures oriented again to the northwest.

The deposition of the conglomerate body of Unit 2 marks a change in the style of sedimentation. Unit 2 was likely linked to tectonic uplift of the southern margin of the Guadalquivir Basin. It is possible that this tectonic arrangement finally caused the closure of the Guadalhorce Corridor (Fig. 11D) (Martín et al., 2001). After that, the Osuna area was affected only by the Atlantic tidal currents reaching the Guadalquivir Basin (Fig. 11E). The morphology of this area, inherited from the previous Guadalhorce Corridor probably limited the flow direction of the tides resulting in the dominant northwest orientation of the sedimentary structures of Unit 3 (Fig. 10E).

6. Conclusions

This work presents a mixed carbonate-siliciclastic contourite drift developed at the northern entrance of the Guadalhorce Corridor, a Messinian seaway connecting the Mediterranean Sea and the Atlantic Ocean through the Guadalquivir Basin in the Betic Cordillera (S Spain). Based on the facies and sedimentary structures, the studied Osuna Quarry section was divided in three units: 1) the lower Unit 1 comprises a 33-m thick succession of large bodies with large-scale cross-stratification pointing to the southeast and secondarily to the northwest; 2) Unit 2 consists of a 2 to 0.5-m thick conglomerate body eroding the top of Unit 1; and 3) Unit 3, is a 6-m thick body with herringbone cross-stratification and a dominant direction of the structures to the northwest.

Unit 1 can be interpreted as a contourite drift deposit due to the occurrence of: 1) up to 10-m thick sediment bodies with planar or through mega cross-bedding; 2) two dominant directions of the sedimentary structures; and 3) reactivation surfaces usually marked by changes in the grain size of the sediment. The two flow directions recorded by the sedimentary structures are related to the position of the contourite drift at the northern end of the coeval Guadalhorce Corridor. The dominance of sedimentary structures pointing to the southeast is the result of the Atlantic inflow into the Mediterranean, while the structures oriented to the northwest record the Mediterranean outflow through the corridor. The dominance of either inflow or outflow waters through the strait was likely modulated by relative sea-level fluctuations. The conglomerate of Unit 2 suggests regional uplift of the southern margin of the Guadalquivir Basin that promoted a turnover in the depositional mode from a bottom-current dominated (Unit 1) to a tide-dominated environment (Unit 3). This tectonic pulse recorded by the increase in the amount and grain size of siliciclastics was likely related to the closure of the Guadalhorce Corridor.

The Osuna Drift indicates for the first time the occurrence of bottom currents related to the Atlantic inflow through the Betic Cordillera during the Messinian which so far were only reported to occur through the Rifian Corridors. This also contradicts the classical "Siphon" model for the Atlantic-Mediterranean bottom-current circulation pattern during the Messinian and sheds light on the complex palaeoceanography during the Late Miocene that predates the Messinian salinity crisis.

References

Aguirre, J., Braga, J.C., Martín, J.M., Puga-Bernabéu, Á., Pérez-Asensio, J.N., Sánchez-Almazo, I.M., Génio, L., 2015. An enigmatic kilometer-scale concentration of small mytilids (Late Miocene, Guadalquivir Basin, S Spain). Palaeogeography, Palaeoclimatology, Palaeoecology 436, 199–213. https://doi.org/10.1016/j.palaeo.2015.07.015.

Anselmetti, F.S., Eberli, G.F., Ding, Z.D., 2000. From the Great Bahama Bank into the Straits of Florida: a margin architecture controlled by sea-level fluctuations and ocean currents. Geological Society of America Bulletin 112, 829–844. https://doi.org/10.1130/0016-7606(2000)112<829:FTGBBI>2.0.CO;2.

Bassi, D., Simone, L, Nebelsick, J.H., 2017. Re-sedimented rhodoliths in channelized depositional systems. In: Riosmena-Rodríguez, R., Nelson, W., Aguirre, J. (Eds.), Rhodolith/Maërl Beds: A Global Perspective. Coastal Research Library 15. Springer, Chambridge, pp. 139–167 https://doi.org/10.1007/978-3-319-29315-8_6.

Benson, R.H., Rakic-El Bied, K., Bonaduce, G., 1991. An important current reversal (influx) in the Rifian Corridor (Morocco) at the Tortonian-Messinian boundary: the end of Tethys Ocean. Paleoceanography 6, 165–192. https://doi.org/10.1029/90PA00756.

Berggren, W.A., Haq, B.U., 1976. The Andalusian stage (Late Miocene): biostratigraphy, biochronology and paleoecology. Palaeogeography, Palaeoclimatology, Palaeoecology 20, 67–129. https://doi.org/10.1016/0031-0182(76)90026-2.

Bergman, K.L., 2004. Seismic Analysis of Paleocurrent Features in the Florida Straits: Insights into the Paleocurrent, Upstream Tectonics, and the Atlantic-Caribbean Connection. Ph.D. thesisUniversity of Miami (190 pp.).

Betzler, C., Braga, J.C., Martín, J.M., Sánchez-Almazo, I.M., Lindhorst, S., 2006. Closure of a seaway: stratigraphic record and facies (Guadix basin, Southern Spain). International Journal of Earth Sciences 95, 903–910. https://doi.org/10.1007/s00531-006-0073-y.

Betzler, C., Lindhorst, S., Eberli, G.P., Lüdmann, T., Möbius, J., Ludwig, J., Schütter, I., Wunsch, M., Reijmer, J.J.G., Hübscher, C., 2014. Periplatform drift: the combined result of contour current and off-bank transport along carbonate platforms. Geology 42, 871–874. https://doi.org/10.1130/G35900.1.

Betzler, C., Eberli, G.P., Kroon, D., Wright, J.D., Swart, P.K., Nath, B.N., Alvarez-Zarkikian, C.A., Alonso-García, M., Bialik, O.M., Blatter, C.L., Guo, J.A., Haffen, S., Horozal, S., Inoue, M., Jovane, L., Lanci, L., Laya, J.C., Mee, A.L., Lüdmann, T., Nakakuni, M., Niino, K., Petruny, L.M., Pratiwi, S.D., Reijmer, J.J.G., Reolid, J., Slagle, A.L., Sloss, C.R., Su, X., Yao, Z., Young, J.R., 2016. The abrupt onset of the modern south Asian monsoon winds. Scientific Reports 6, 29838. https://doi.org/10.1038/srep29838.

Betzler, C., Eberli, G.P., Lüdmann, T., Reolid, J., Kroon, D., Reijmer, J.J.G., Swart, P.K., Wright, J.D., Young, J.R., Alvarez-Zarikian, C.A., Alonso-García, M., Bialik, O.M., Blattler, C.L., Guo, J.A., Haffen, S., Horozal, S., Inoue, M., Jovane, L., Lanci, L., Laya, J.C., Mee, A.L.H., Nakakuni, M., Nath, B.N., Niino, K., Petruny, L.M., Pratiwi, S.D., Slagle, A.L., Sloss, C.R., Su, X., Yao, Z., 2018. Refinement of Miocene sea level and monsoon events from the sedimentary archive of the Maldives (Indian Ocean). Progress in Earth and Planetary Science 5. https://doi.org/10.1186/s40645-018-0165-x.

Bialik, O.M., Reolid, J., Kulhanek, D., Hincke, C., Waldmann, N., Betzler, C., 2022. Sedimentary response to current and nutrient regime rearrangement in the Eastern Mediterranean Realm during the early to middle Miocene (southwestern Cyprus). Palaeogeography, Palaeoclimatology, Palaeoecology 588, 110819. https://doi.org/10.1016/j.palaeo.2021.110819.

BouDagher-Fadel, M.K., 2015. Biostratigraphic and Geological Significance of Planktonic Foraminifera. UCLPress, London (306 pp.) http://www.jstor.org/stable/j.ctt1g69xwk.

Braga, J.C., Martín, J.M., Aguirre, J., 2002. Tertiary. In: Gibbons, W., Moreno, T. (Eds.), The Geology of Spain. Southern Spain. Geological Society, London, pp. 320–327 https://doi.org/10.1144/GOSPP.13.

Bunzel, D., Schmiedls, G., Lindhorst, S., Mackensen, A., Reolid, J., Romahn, S., Betzler, C., 2017. A multi-proxy analysis of Late Quaternary ocean and climate variability for the Maldives, Inner Sea. Climate of the Past 13, 1791–1813. https://doi.org/10.5194/cp-13-1791-2017.

Capella, W., Barhoun, N., Flecker, R., Hilgen, F.J., Kouwenhoven, T., Matenco, L.C., Krijgsman, W., 2018. Data on lithofacies, sedimentology and palaeontology of South Rifian Corridor sections (Morocco). Data in Brief 19, 712–736. https://doi.org/10.1016/j.dib.2018.05.047.

Chabaud, L., Ducassou, E., Tournadour, E., Mulder, T., Reijmer, J.J.G., Conesa, G., Giraudeau, J., Hanquiez, V., Borgomano, J., Ross, L., 2016. Sedimentary processes determining the

modern carbonate periplatform drift of Little Bahama Bank. Marine Geology 378, 213–229. https://doi.org/10.1016/j.margeo.2015.11.006.

CloudCompare, 2021. 3D point cloud and mesh processing software. Open Source Project CloudCompare (version 2.11.3).

Coletti, G., Basso, D., Frixa, A., Corselli, C., 2015. Transported rhodoliths witness the lost carbonate factory: a case history from the Miocene Pietra da Cantoni limestone (NW Italy). Rivista Italiana di Paleontologia e Stratigrafia 121 (3). https://doi.org/10.13130/2039-4942/6522.

Cruz-Sanjulián, J., 1975. Estudio geológico del sector Cañete la Real-Teba-Osuna (Cordillera bética, región occidental). PhD ThesisUniversidad de Granada (431 pp.). (in Spanish).

Davis, R.A., 2012. Tidal signatures and their preservation potential in stratigraphic sequences. In: Davis, R.A., Dalrymple, R.W. (Eds.), Principles of Tidal Sedimentology New York. Springer, pp. 35–56 https://doi.org/10.1007/978-94-007-0123-6_3 (625, pp.).

de Castro, S., Miramontes, E., Dorador, J., Jouet, G., Cattaneo, A., Rodríguez-Tovar, F.J., Hernández-Molina, F.J., 2021. Siliciclastic and bioclastic contouritic sands: textural and geochemical characterisation. Marine and Petroleum Geology 128, 105002. https://doi.org/10.1016/j.marpetgeo.2021.105002.

de Weger, W., Hernández-Molina, F.J., Miguez-Salas, O., de Castro, S., Bruno, M., Chiarella, D., Sierro, F.J., Blackbourn, G., Manar, M.A., 2021. Contourite depositional system after the exit of a strait: case study from the late Miocene South Rifian Corridor, Morocco. Sedimentology 68, 2996–3032. https://doi.org/10.1111/sed.12882.

Divar, J., Cruz-Sanjulián, J., 1986. Mapa Geológico de España a Escala 1:50.000. Explicación de la hoja 1005 (15–41) Osuna. Instituto Geológico Minero de España. Ministerio de Industria, Madrid (in Spanish).

Eberli, G.P., Betzler, C., 2019. Characteristics of modern carbonate contourite drifts. Sedimentology 66, 1163–1191. https://doi.org/10.1111/sed.12584.

Eberli, G.P., Bernoulli, D., Vecsei, A., Sekti, R., Grasmueck, M., Lüdmann, T., Della Porta, G., 2019. A Cretaceous carbonate delta drift in the Montagna della Maiella, Italy. Sedimentology 66, 1266–1301. https://doi.org/10.1111/sed.12590.

Ercilla, G., Baraza, J., Alonso, B., Estrada, F., Casas, D., Farrán, M., 2002. The Ceuta Drift, Alboran Sea (southwestern Mediterranean). In: Stow, D.A.V., Pudsey, C.J., Howe, J. A., Faugères, J.-C., Viana, A.R. (Eds.), Deep-Water Contourite Systems: Modern Drifts and Ancient Series, Seismic and Sedimentary Characteristics. Geological Society, London, Memoirvol. 22, pp. 155–170. https://doi.org/10.1144/GSL.MEM.2002.022.01.12.

Flecker, R., Krijgsman, W., Capella, W., Martins, C., Dmitrieva, E., Mayser, J.P., Marzocchi, A., Modestu, S., Ochoa, D., Simon, D., Tulbure, M.A., Berg, B.V., Schee, M.V., Lange, G.J., Ellam, R.M., Govers, R., Gutjahr, M., Hilgen, F.J., Kouwenhoven, T.J., Lofi, J., Meijer, P.T., Sierro, F.J., Bachiri, N., Barhoun, N., Alami, A.C., Chacón, B., Flores, J., Gregory, J.M., Howard, J.P., Lunt, D.J., Ochoa, M., Pancost, R.D., Vincent, S., Yousfi, M.Z., 2015. Evolution of the Late Miocene Mediterranean–Atlantic gateways and their impact on regional and global environmental change. Earth-Science Reviews 150, 365–392. https://doi.org/10.1016/j.earscirev.2015.08.007.

Galindo-Zaldívar, J., Braga, J.C., Marín-Lechado, C., Ercilla, G., Martín, J.M., Pedrera, A., Alonso, B., 2019. Extension in the Western Mediterranean. In: Quesada, C., Oliveira, J.T. (Eds.), The Geology of Iberia: A Geodynamic Approach. Springer, Chambridge, pp. 61–103.

García-Castellanos, D., Fernández, M., Torné, M., 2002. Modelling the evolution of the Guadalquivir foreland basin (southern Spain). Tectonics 21. https://doi.org/10.1029/2001TC001339 (9–1).

García-Gallardo, Á., Grunert, P., Van der Schee, M., Sierro, F.J., Jiménez-Espejo, F.J., Alvarez Zarikian, C.A., Piller, W.E., 2017. Benthic foraminifera-based reconstruction of the first Mediterranean-Atlantic exchange in the early Pliocene Gulf of Cadiz. Palaeogeography, Palaeoclimatology, Palaeoecology 472, 93–107. https://doi.org/10.1016/j.palaeo.2017.02.009.

Gonthier, E., Faugères, J.C., Stow, D.A.V., 1984. Fine grained sediments, deep-water processes and facies. In: Stow, D.A.V., Piper, D.J.W. (Eds.), Geological Society of London, Special Publicationvol. 15, pp. 275–291.

González-Delgado, J.A., Civis, J., Dabrio, C.J., Goy, J.L., Ledesma, S., Pais, J., Sierro, F.J., Zazo, C., 2004. Cuenca del Guadalquivir. In: Vera, J.A. (Ed.), Geología de España. SGE-IGME, Madrid, pp. 543–550 (in Spanish).

Harris, P.T., Tsuji, Y., Marshall, J.F., Davies, P.J., Honda, N., Matsuda, H., 1996. Sand and rhodolith-gravel entrainment on the mid- to outer-shelf under a western boundary current: Fraser Island continental shelf, eastern Australia. Marine Geology 129, 313–330. https://doi.org/10.1016/0025-3227(96)83350-0.

Hernandez-Molina, F.J., Llave, E., Stow, D.A.V., Garcia, M., Somoza, L., Vazquez, J.T., Lobo, F.J., Maestro, A., del Rio, V.D., Leon, R., Medialdea, T., Gardner, J., 2006. The contourite depositional system of the Gulf of Cadiz: a sedimentary model related to the bottom current activity of the Mediterranean outflow water and its interaction with the continental margin. Deep-Sea Research Part II: Topical Studies in Oceanography 53, 1420–1463. https://doi.org/10.1016/j.dsr2.2006.04.016.

Hernández-Molina, F.J., Stow, D.A.V., Llave, 2008. Continental slope contourites. In: Rebesco, M., Camerlenghi, A. (Eds.), Contourites. Developments in Sedimentologyvol. 60. Elsevier, Amsterdam, pp. 379–408. https://doi.org/10.1016/S0070-4571(08)10019-X.

Hernández-Molina, F.J., Serra, N., Stow, D.A.V., Llave, E., Ercilla, G., Van Rooij, D., 2011. Along-slope oceanographic processes and sedimentary products around the Iberian margin. Geo-Marine Letters 31, 315–341. https://doi.org/10.1007/s00367-011-0242-2.

Hernández-Molina, F.J., Stow, D.A.V., Alvarez-Zarikian, C., Expedition IODP 339 Scientists, 2013. IODP Expedition 339 in the Gulf of Cadiz and offWest Iberia: decoding the environmental significance of the Mediterranean Outflow Water and its global influence. Scientific Drilling 16, 1–11. https://doi.org/10.5194/sd-16-1-2013.

Hernández-Molina, F.J., Llave, E., Preu, B., Ercilla, G., Fontan, A., Bruno, M., Serra, N., Gomiz, J.J., Brackenridge, R.E., Sierro, F.J., Stow, D.A.V., García, M., Juan, C., Sandoval, N., Arnaiz,

A., 2014. Contourite processes associated to the Mediterranean Outflow Water after its exit from the Gibraltar Strait: global and conceptual implications. Geology 42, 227–230. https://doi.org/10.1130/G35083.1.

Holbourn, A., Henderson, A.S., MacLeod, N., 2013. Atlas of Benthic Foraminifera. Blackwell, Willey (642 pp.).

Huneke, N.V., Stow, D.A.V., 2008. Identification of ancient contourites: problems and palaeoceanographic significance. In: Rebesco, M., Camerlenghi, A. (Eds.), Contourites. Developments in Sedimentologyvol. 60, pp. 323–344. https://doi.org/10.1016/S0070-4571(08)10017-6.

Hüneke, H., Hernández-Molina, F.J., Rodríguez-Tovar, F.J., Llave, E., Chiarella, D., Mena, A., Stow, D.A., 2020. Diagnostic criteria using microfacies for calcareous contourites, turbidites and pelagites in the Eocene-Miocene slope succession, southern Cyprus. Sedimentology 68, 557–592. https://doi.org/10.1111/sed.12792.

Jiménez-Moreno, G., Pérez-Asensio, J.N., Larrasoaña, J.C., Aguirre, J., Civis, J., Rivas-Carballo, M.R., Valle-Hernández, M.F., González-Delgado, J.A., 2013. Vegetation, sea-level and climate changes during the Messinian salinity crisis. Geological Society of America Bulletin 125, 432–444. https://doi.org/10.1130/B30663.1.

Kennett, J.P., Srinivasan, M.S., 1983. Neogene Planktonic Foraminifera, a Phylogenetic Atlas. Hutchinson Ross, Stroudsburg, Pennsylvania (265 pp.).

Klein, G.D., 1970. Depositional and dispersal dynamics of intertidal sand bars. Journal of Sedimentary Research 40, 1095–1127.

Krijgsman, W., Capella, W., Simon, D., Hilgen, F.J., Kouwenhoven, T.J., Meijer, P.T.H., Sierro, F.J., Tulbure, M.A., van den Berg, B.C.J., van der Schee, M., Flecker, R., 2018. The Gibraltar Corridor: watergate of the Messinian salinity crisis. Marine Geology 403, 238–246. https://doi.org/10.1016/j.margeo.2018.06.008.

Larrasoaña Gorosquieta, J.C., Sierro, F.J., Mata Campo, M.P., van den Berg, B.C., Pérez-Asensio, J.N., Salazar Rincón, Á.E., Salvany, J.M., Ledesma, S., García-Castellanos, D., Civis Llovera, J., Cunha, P.P., 2019. Guadalquivir Basin. In: Quesada, C., Oliveira, J.T. (Eds.), The Geology of Iberia: A Geodynamic Approach. Springer, Chambridge, pp. 61–103.

Lima, J.A.M., Moeller, O.O., Viana, A.R., Piovesan, R., 2007. Hydrodynamic modelling of bottom currents and sediment transport in the Canyon Sao Tome (Brazil). In: Viana, A.R., Rebesco, M. (Eds.), Economic and Palaeoceanographic Significance of Contourites. Geological Society, London, Special Publicationvol. 276, pp. 329–342. https://doi.org/10.1144/GSL.SP.2007.276.01.16.

Longhitano, S.G., Chiarella, D., 2020. Chapter 15 – tidal straits: basic criteria for recognizing ancient systems from the rock record. In: Scarselli, N., Adam, J., Chiarella, D., Roberts, D.G., Bally, A.W. (Eds.), Regional Geology and Tectonics. vol. 1. Principles of Geologic Analysis. Elsevier, Amsterdam, pp. 365–415. https://doi.org/10.1016/B978-0-444-64134-2.00014-6.

Longhitano, S.G., Chiarella, D., Muto, F., 2014. Three-dimensional to two-dimensional cross-strata transition in the lower Pleistocene Catanzaro tidal strait transgressive succession (southern Italy). Sedimentology 61, 2136–2171. https://doi.org/10.1111/sed.12138.

López-Garrido, A.C., Sanz de Galdeano, C.C., 1999. Neogene sedimentation and tectonic-eustatic control of the Málaga Basin, South Spain. Journal of Petroleum Geology 22, 81–96.

Lüdmann, T., Paulat, M., Betzler, C., Möbius, J., Lindhorst, S., Wunsch, M., Eberli, G.P., 2016. Carbonate mounds in the Santaren Channel, Bahamas: a current-dominated periplatform depositional regime. Marine Geology 376, 69–85. https://doi.org/10.1016/j.margeo.2016.03.013.

Lüdmann, T., Betzler, C., Eberli, G.P., Reolid, J., Reijmer, J.J.G., Sloss, C.R., Bialik, O.M., Alvarez-Zarkikian, C.A., Alonso-Garcia, M., Blatter, C.L., Guo, J.A., Haffen, S., Horozal, S., Inoue, M., Jovane, L., Kroon, D., Lanci, L., Laya, J.C., Mee, A.L., Nakakuni, M., Nath, B.N., Niino, K., Petruny, L.M., Pratiwi, S.D., Slagle, A.L., Su, X., Swart, P.K., Wright, J.D., Yao, Z., Young, J.R., 2018. Carbonate delta drifts: a new drift type. Marine Geology 401, 98–111. https://doi.org/10.1016/j.margeo.2018.04.011.

Lutze, G.F., Thiel, H., 1989. Epibenthic foraminifera from elevated microhabitats: Cibicidoides wuellerstorfi and Planulina ariminensis. Journal of Foraminiferal Research 19, 153–158.

Marrack, E.C., 1999. The relationship between water motion and living Rhodolith beds in the Southwestern Gulf of California, Mexico. Palaios 14, 159–171.

Martín, J.M., Braga, J.C., Betzler, C., 2001. The Messinian Guadalhorce corridor: the last northern, Atlantic–Mediterranean gateway. Terra Nova 13, 418–424. https://doi.org/10.1046/j.1365-3121.2001.00376.x.

Martín, J.M., Braga, J.C., Aguirre, J., Puga-Bernabéu, Á., 2009. History and evolution of the North-Betic Strait (Prebetic Zone, Betic Cordillera): a narrow, early Tortonian, tidal-dominated, Atlantic–Mediterranean marine passage. Sedimentary Geology 216, 80–90. https://doi.org/10.1016/j.sedgeo.2009.01.005.

Martín, J.M., Braga, J.C., Sánchez-Almazo, I.M., Aguirre, J., 2010. Temperate and tropical carbonate-sedimentation episodes in the Neogene Betic basins (southern Spain) linked to climatic oscillations and changes in Atlantic-Mediterranean connections: constraints from isotopic data. In: Mutti, M., Piller, W., Betzler, C. (Eds.), Carbonate Systems during the Oligocene-Miocene Climatic Transition. vol. 42. International Association of Sedimentologists Special Publication, pp. 49–70. https://doi.org/10.1002/9781118398364.ch4.

Martín, J.M., Puga-Bernabéu, Á., Aguirre, J., Braga, J.C., 2014. Miocene Atlantic-Mediterranean seaways in the Betic Cordillera (Southern Spain). Revista Sociedad Geologica de España 27, 175–186.

Martín-Chivelet, J., Fregenal-Martínez, M.A., Chacón, B., 2003. Mid-depth calcareous contourites in the latest Cretaceous of Caravaca (Subbetic Zone, southeast Spain). Origin and paleohydrological significance. Sedimentary Geology 163, 131–146. https://doi.org/10.1016/S0037-0738(03)00176-3.

Martín-Chivelet, J., Fregenal Martínez, M.A., Chacón, B., 2008. Traction structures in contourites. In: Rebesco, M., Camerlenghi, A. (Eds.), Contourites. Developments in

Sedimentology60. Elsevier, Amsterdam, pp. 159–181. https://doi.org/10.1016/S0070-4571(08)10010-3.

Martínez del Olmo, W., 2019. El complejo olistostrómico del Mioceno de la Cuenca del Río Guadalquivir (SO de España). Revista de la Sociedad Geológica de España 32, 3–16 (In Spanish).

Martínez del Olmo, W., Martín, D., 2016. El Neógeno de la cuenca Guadalquivir-Cádiz (Sur de España). Revista de la Sociedad Geológica de España 29, 35–58 (in Spanish).

Millot, C., 2014. Heterogeneities of in-and out-flows in the Mediterranean Sea. Progress in Oceanography 120, 254–278. https://doi.org/10.1016/j.pocean.2013.09.007.

Mullins, H.T., Neumann, H.C., 1979. Geology of the Miami Terrace and its paleo- oceanographic implications. Marine Geology 30, 205–232.

Mullins, H.T., Neumann, A.C., Wilber, R.J., Hine, A.C., Chinburg, A.J., 1980. Carbonate sediment drifts in northern Straits of Florida. Bulletin of the American Association of Petroleum Geologists 64, 1701–1717.

Murray, J.W., 1991. Ecology and Palaeoecology of Benthic Foraminifera. Longman Scientific & Technical, UK (397 pp.).

Murray, J.W., 2006. Ecology and Applications of Benthic Foraminifera. Cambridge University Press, Cambridge (426 pp.).

Nelson, C.S., 1988. An introductory perspective on nontropical shelf carbonates. Sedimentary Geology 60, 3–12.

Nelson, C.H., Baraza, J., Maldonado, A., Rodero, J., Escutia, C., Barber, J.H., 1999. Influence of the Atlantic inflow and Mediterranean outflow currents on Late Quaternary sedimentary facies of the Gulf of Cadiz continental margin. Marine Geology 155, 99–129.

Ng, Z.L., Hernández-Molina, F.J., Duarte, D., Sierro, F.J., Ledesma, S., Llave, C., Roque, C., Manar, M., 2021. Latest Miocene restriction of the Mediterranean Outflow Water: a perspective from the Gulf of Cádiz. Geo-Marine Letters 41, 23. https://doi.org/10.1007/s00367-021-00693-9.

Paulat, M., Lüdmann, T., Betzler, C., Eberli, G.P., 2019. Neogene palaeoceanographic changes recorded in a carbonate contourite drift (Santaren Channel, Bahamas). Sedimentology 66, 1361–1385. https://doi.org/10.1111/sed.12573.

Pérez-Asensio, J.N., 2021. Quantitative palaeobathymetric reconstructions based on foraminiferal proxies: a case study from the Neogene of south-west Spain. Palaeontology 64, 475–488. https://doi.org/10.1111/pala.12538.

Pérez-Asensio, J.N., Aguirre, J., Schmiedl, G., Civis, J., 2012. Impact of restriction of the Atlantic–Mediterranean gateway on the Mediterranean Outflow Water and eastern Atlantic circulation during the Messinian. Paleoceanography 27, PA3222. https://doi.org/10.1029/2012PA002309.

Pérez-Asensio, J.N., Aguirre, J., Jiménez-Moreno, G., Schmiedl, G., Civis, J., 2013. Glacioeustatic control on the origin and cessation of the Messinian salinity crisis. Global and Planetary Change 111, 1–8. https://doi.org/10.1016/j.gloplacha.2013.08.008.

Pérez-Asensio, J.N., Aguirre, J., Schmiedl, G., Civis, J., 2014. Messinian productivity changes in the northeastern Atlantic and their relationship to the closure of the Atlantic–Mediterranean gateway: implications for Neogene palaeoclimate and palaeoceanography. Journal of the Geological Society 171, 389–400. https://doi.org/10.1144/jgs2013-032.

Pérez-Asensio, J.N., Aguirre, J., Rodríguez-Tovar, F.J., 2017. The effect of bioturbation by polychaetes (Opheliidae) on benthic foraminiferal assemblages and test preservation. Palaeontology 60, 807–827. https://doi.org/10.1111/pala.12317.

Puga-Bernabéu, Á., Braga, J.C., Aguirre, J., Martín, J.M., 2022. Sedimentary dynamics and topographic controls on the tidal-dominated Zagra Strait, Early Tortonian, Betic Cordillera, Spain. In: Rossi, V.M., Longhitano, S., Olariu, C., Chiocci, F. (Eds.), Straits and Seaways: Controls, Processes and Implications in Modern and Ancient Systems. Geological Society of London, Special Publications523. https://doi.org/10.1144/SP523-2021-85.

Rebesco, M., 2005. Contourites. In: Selly, R.C., Cocks, L.R.M., Plime, L.R. (Eds.), Encyclopedia of Geology 4. Elsevier, Oxford, pp. 513–527.

Rebesco, M., Hernández-Molina, F.J., Van Rooij, D., Wählin, A., 2014. Contourites and associated sediments controlled by deep-water circulation processes: state-of-the-art and future considerations. Marine Geology 352, 111–154. https://doi.org/10.1016/j.margeo.2014.03.011.

Reolid, J., Betzler, C., 2019. The ichnology of carbonate drifts. Sedimentology 66, 1427–1448. https://doi.org/10.1111/sed.12563.

Reolid, M., García-García, F., Reolid, J., de Castro, A., Bueno, J.F., Martín-Suárez, E., 2016a. Palaeoenvironmental interpretation of a sand-dominated coastal system of the Upper Miocene of eastern Guadalquivir Basin (south Spain): fossil assemblages, ichnology and taphonomy. Journal of Iberian Geology 42, 275–290. https://doi.org/10.5209/jige.52886.

Reolid, J., Betzler, C., Braga, J.C., 2016b. Amplitude of lateMiocene sea-level fluctuations from karst development in reef-slope deposits (SE Spain). Sedimentary Geology 345, 145–153. https://doi.org/10.1016/j.sedgeo.2016.09.009.

Reolid, J., Betzler, C., Lüdmann, T., 2019. Facies and sedimentology of a carbonate delta drift (Miocene, Maldives). Sedimentology 66, 1243–1265. https://doi.org/10.1111/sed.12575.

Reolid, J., Betzler, C., Bialik, O.M., Waldman, N., 2021. Lenticular-bedding-like bioturbation and the onshore recognition of carbonate drifts (Oligocene, Cyprus). Journal of Sedimentary Research 90, 1667–1677. https://doi.org/10.2110/jsr.2020.70.

Rodríguez-Tovar, F.J., Hernández-Molina, F.J., 2018. Ichnological analysis of contourites: past, present and future. Earth-Science Reviews 182, 28–41. https://doi.org/10.1016/j.earscirev.2018.05.008.

Schönfeld, J., 1997. The impact of the Mediterranean outflow water (MOW) on benthic foraminiferal assemblages and surface sediments at the southern Portuguese continental margin. Marine Micropaleontology 29, 211–236.

Schönfeld, J., 2002a. A new benthic foraminiferal proxy for near-bottom current velocities in the Gulf of Cadiz, northeastern Atlantic Ocean. Deep-Sea Research Part I Oceanographic Research Paper 49, 1853–1875. https://doi.org/10.1016/S0967-0637(02)00088-2.

Schönfeld, J., 2002b. Recent benthic foraminiferal assemblages in deep high-energy environments from the Gulf of Cadiz (Spain). Marine Micropaleontology 44, 141–162.

Shanmugam, G., 2000. 50 years of the turbidite paradigm (1950s–1990s): deep-water processes and facies models: a critical perspective. Marine and Petroleum Geology 17, 285–342. https://doi.org/10.1016/S0377-8398(01)00039-1.

Shanmugam, G., 2008. Deep-water bottom currents and their deposits. In: Rebesco, M., Camerlenghi, A. (Eds.), Contourites, Developments in Sedimentology 60. Elsevier, Amsterdam, pp. 59–81 https://doi.org/10.1016/S0070-4571(08)10005-X.

Shanmugam, G., 2017. Contourites: physical oceanography, process sedimentology, and petroleum geology. Petroleum Exploration and Development 44, 183–216. https://doi.org/10.1016/S1876-3804(17)30023-X.

Shanmugam, G., Spalding, T.D., Rofheart, D.H., 1993a. Process sedimentology and reservoir quality of deep-marine bottom-current reworked sands (sandy contourites): an example from the Gulf of Mexico. American Association of Petroleum Geologists Bulletin 77, 1241–1259.

Shanmugam, G., Spalding, T.D., Rofheart, D.H., 1993b. Traction structures in deep-marine bottom-current reworked sands in the Pliocene and Pleistocene, Gulf of Mexico. Geology 21, 929–932.

Soto-Navarro, J., Criado-Aldeanueva, F., García-Lafuente, J., Sánchez-Román, A., 2010. Estimation of the Atlantic inflow through the Strait of Gibraltar from climatological and in situ data. Journal of Geophysical Research: Oceans 115, C10023. https://doi.org/10.1029/2010JC006302.

Stow, D.A.V., Faugères, J.C., 2008. Chapter 13: contourite facies and the facies model. In: Rebesco, M., Camerlenghi, A. (Eds.), Contourites, Developments in Sedimentology 60. Elsevier, Amsterdam, pp. 223–256 https://doi.org/10.1016/S0070-4571(08)10013-9.

Stow, D.A.V., Smillie, Z., 2020. Distinguishing between deep-water sediment facies: turbidites, contourites and hemipelagites. Geoscience 10, 68. https://doi.org/10.3390/geosciences10020068.

Stow, D.A.V., Faugères, J.C., Viana, A.R., Gonthier, E., 1998. Fossil contourites: a critical review. Sedimentary Geology 115, 3–31. https://doi.org/10.1016/S0037-0738(97)00085-7.

Stow, D.A.V., Kahler, G., Reeder, M., 2002. Fossil contourites: Type example from an Oligocene palaeoslope system, Cyprus. In: Stow, D.A.V., Pudsey, C.J., Howe, J.A., Faugéres, J.C., Viana, A.R. (Eds.), Deep-Water Contourite Systems: Modern Drifts and Ancient Series, Seismic and Sedimentary Characteristics. Geological Society of London Memoirsvol. 22, pp. 443–455. https://doi.org/10.1144/GSL.MEM.2002.022.

Stow, D.A.V., Hernández-Molina, F.J., Llave, E., Sayago-Gil, M., Diaz-del Rio, V., Branson, A., 2009. Bedform-velocity matrix: the estimation of bottom current velocity from bedform observations. Geology 37, 327–330. https://doi.org/10.1130/G25259A.1.

Tulbure, M.A., Capella, W., Barhoun, N., Flores, J.A., Hilgen, F.J., Krijgsman, W., Kouwenhoven, T., Sierro, F.J., Yousfi, M.Z., 2017. Age refinement and basin evolution of the North Rifian Corridor (Morocco): no evidence for a marine connection during the Messinian Salinity Crisis. Palaeogeography, Palaeoclimatology, Palaeoecology 485, 416–432. https://doi.org/10.1016/j.palaeo.2017.06.031.

Van der Zwaan, G.J., Jorissen, F.J., de Stigter, H.C., 1990. The depth dependency of planktonic/benthic foraminiferal ratios: constraints and applications. Marine Geology 95, 1e16. https://doi.org/10.1016/0025-3227(90)90016-D.

Van Morkhoven, F.P.C.M., Berggren, W.A., Edwards, A.S., 1986. Cenozoic cosmopolitan deep-water benthic foraminifera. Bulletin des Centres de Recherches Exploration-Production Elf-Aquitaine: Mémoire 11 (421 pp.).

Verdenius, J.G., 1970. Neogene stratigraphy of the western Guadalquivir Basin (southern Spain). Phd thesisUtrecht University (109 pp.).

Viana, A.R., 2001. Seismic expression of shallow- to deep-water contourites along the south-eastern Brazilian margin. Marine Geophysical Research 22, 509–521. https://doi.org/10.1023/A:1016307918182.

Wetzel, A., Werner, F., Stow, D.A.V., 2008. Bioturbation and biogenic sedimentary structures in contourites. In: Rebesco, M., Camerlenghi, A. (Eds.), Contourites. Developments in Sedimentologyvol. 60. Elsevier, Amsterdam, pp. 183–202. https://doi.org/10.1016/S0070-4571(08)10011-5.

Wüst, G., 1961. On the vertical circulation of the Mediterranean Sea. Journal of Geophysical Research 66, 3261–3271.